PREDICTION OF AERODYNAMIC COEFFICIENTS OF FORCE AND MOMENT ACTING ON BODIES OF REVOLUTION

48

12

1

A THESIS

Submitted in partial fulfillment
of the requirements for the Degree
of Master of Science in Aeronautical Engineering

by

Hurlbut William Smith LaVier

Georgia School of Technology
Atlanta, Georgia
1947

PREDICTION OF AERODYNAMIC COEFFICIENTS OF FORCE

AND MOMENT ACTING ON BODIES OF REVOLUTION

Approved:

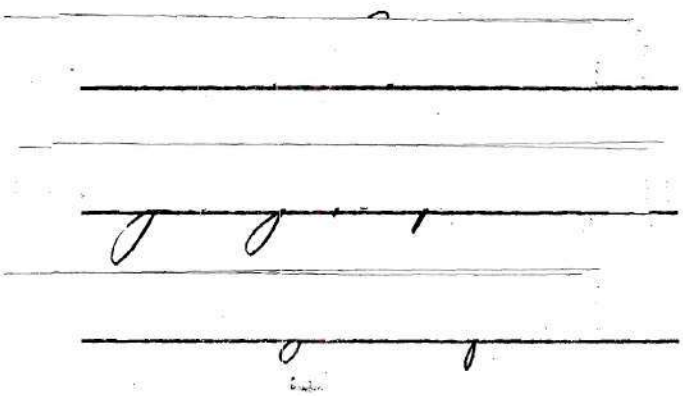

Date Approved by Chairman June 9th 1947

ACKNOWLEDGMENTS

The cooperation of Professor Alan Y. Pope, serving in the dual capacity of Thesis Advisor and Chairman of the Committee, is greatfully appreciated by the author. Also, thanks are extended to Professors W. B. Johns and J. J. Harper, who were kind enough to serve on the Committee.

Professor George K. Williams was of great service to the author, lending encouragement during some of the darkest hours of thesis preparation.

TABLE OF CONTENTS

PAGE

Approval Sheet..... ii

Acknowledgments..... iii

List of Tables..... v

List of Figures..... vi

Summary..... 1

Introduction..... 3

Review of the Literature..... 4

Development of the Procedure..... 26

Prediction of Normal Force..... 26

Prediction of Moment..... 28

Prediction of Drag..... 30

Demonstration of Procedure..... 33

Conclusions..... 39

BIBLIOGRAPHY..... 40

TABLES..... 43

FIGURES..... 62

LIST OF TABLES

TABLE		PAGE
I.	Spheroidal Properties, L/D = 1.0	44
II.	Spheroidal Properties, L/D = 2.0	45
III.	Spheroidal Properties, L/D = 3.0	46
IV.	Spheroidal Properties, L/D = 4.0	47
V.	Spheroidal Properties, L/D = 4.5	48
VI.	Spheroidal Properties, L/D = 5.0	49
VII.	Spheroidal Properties, L/D = 7.0	50
VIII.	Spheroidal Properties, L/D =10.0	51
IX.	y Sin2 α Correction Factors	52
X.	Distribution of y Sin2 α, Corrected	53
XI.	Variation of $\frac{\pi AB}{2} \sum$ y Sin2 α with Fineness Ratio	54
XII.	Determination of Angle of Attack Correction Factor K_θ	55
XIII.	Comparison of Computed and Measured Pitching Moment of a Prolate Spheroid, L/D = 4.0	56
XIV.	Force and Moment Coefficients for a Cylindrical Body of Revolution in the Nine Foot Wind Tunnel	57
XV.	Predicted Normal Force and Moment Coefficients	58
XVI.	Determining Projected Frontal Area	59
XVII.	Computation of the Predicted Drag Coefficients	60
XVIII.	Conversion of C_N and C_D (Predicted) into C_c	61

LIST OF FIGURES

FIGURE		PAGE
1.	Prolate Spheroid in Oblique Flow	63
2.	Karman's Method for Computing Pressure Distributions	64
3.	Karman's Method, Transverse Force Distribution	65
4.	Lamb's Inertia Coefficients for the Prolate Spheroid	66
5.	Symbols for the Prolate Spheroid Theories	67
6.	Comparison of Theoretical with Experimental Transverse Force Distributions for Prolate Spheroid	68
7.	Distribution of y Sin2 α	69
8.	Variation of $\pi \frac{AB}{2} \sum y \sin 2\alpha$	70
9.	Angle of Attack Correction Factor K_θ	71
10.	Body of Revolution Tested in the Nine Foot Wind Tunnel	72
11.	Comparison of Inertia Coefficients, Prolate Spheroid with Cylinder	73
12.	Force Diagram, Body of Revolution Tested in Nine Foot Wind Tunnel	74
13.	Coefficients of Lift, Drag, and Moment for Body of Revolution Tested in Nine Foot Wind Tunnel	75
14.	Comparison of Predicted with Measured Values of C_N, C_c, and C_D for Body of Revolution Tested in Nine Foot Wind Tunnel	76

PREDICTION OF AERODYNAMIC COEFFICIENTS OF FORCE AND MOMENT ACTING ON BODIES OF REVOLUTION

SUMMARY

The object of this thesis is to develop a practical procedure for the prediction of aerodynamic forces and moments acting on bodies of revolution. Study of various pertinent theories and procedures developed in connection with airship design reveal them to be cumbersome and of little practical use for design and development purposes.

In extracting a practical procedure for analytical prediction of aerodynamic forces and moments acting on bodies of revolution, it was found that no one procedure would yield lift, drag, and moment. Furthermore, it was necessary to compare pressure and transverse force distributions obtained both by theory and experiment in order that theoretical results might be rendered consistent with those obtained through experiment.

Study of pertinent literature suggested the idea that the wake and fluid mass in the forward "deadwater region" resulting from a flow of real fluid about a bluff body in effect acts as though rigidly attached to the body, and in combination approximates a shape consistent with requirements of potential flow. From this it logically followed to utilize theories pertinent to flow about prolate spheroids of various fineness ratios. Result of this is a practical procedure for the analytical prediction of aerodynamic forces of lift, drag, moment acting on any body of revolution. As regards lift and moment, the procedure

is essentially that of choosing an equivalent spheroid having the same apparent mass effects. However, in the case of drag excellent results are obtained by computing the head pressures and adding to it a quantity representative of the drag resulting from skin friction.

INTRODUCTION

High speed flight has resulted in reduction of wing area to a minimum. Consequently, the aerodynamic forces and moments acting on the airplane fuselage or body can no longer be neglected. Their magnitude is comparable to the forces and moments acting on the wings.

The analytical prediction of aerodynamic forces and moments for airfoil shapes has been thoroughly developed and close agreement between theory and test results may be obtained. However, the three dimensional problem concerning bodies of revolution has not been developed to the same degree. There is no question concerning the importance and the need for a practical procedure for predicting these forces and moments for bodies of revolution in advance of, or in absence of wind tunnel tests.

REVIEW OF THE LITERATURE

The two dimensional problem of computing the velocity distribution about an airfoil has been thoroughly considered and several precise procedures are currently used. Representative of these, and perhaps the best, is the method developed by Dr. Theodorsen[1] based on potential field theory principles.

In three dimensions the problem of flowabout shapes of revolution was the subject of considerable study on the part of early students of hydro-aeromechanics. However, in the light of modern consideration of the problem it is disappointing that their studies were directed almost entirely to the determination of resistance of such bodies and to the characteristics of the flow of an ideal fluid about the bodies. An idea of the nature and extent of this consideration is found in a book by Prandtl-Tietjens[2]. Shapes thus considered consisted of cylindrical shapes with hemispherical forebody or nosepiece, and streamlined or "tear" shaped bodies of revolution.

Development of the airship or dirigible, lighter than aircraft depending upon buoyancy for lift, necessitated a careful study of the dynamics of the airship in flight, which in turn made it necessary to consider the aerodynamic moments and cross force (or lift) as well as the drag. The familiar dirigible or airship hull is a modification of

---

[1] T. Theodorsen and I. E. Garrick, "General Potential Theory of Arbitrary Wing Sections", National Advisory Committee for Aeronautics Technical Report 452, 1933.

[2] Prandtl-Tietjens, "Applied Hydro and Aeromechanics", McGraw-Hill and Company, 1934.

the teardrop or an elongated prolate spheroid shape. As a result of this close approximation to the ellipsoidal shape, mathematical treatment of the flow problem is facilitated. Prandtl-Tietjen[2] advises that a streamlined or "tear" shaped body, familiar airship hull shape, is the only body of revolution for which the actual flow around the body is almost identical to the computed flow for the same shape in an ideal fluid. This is the reason why the two-dimensional airfoil procedures and the several developed for use with airship hull shapes are successfully used in practice.

A. F. Zahm[3] presents formulas that may be used to compute the pressure distribution about and resistance of simple quadrics fixed in an infinite uniform stream of practically incompressible fluid. The quadrics considered include the sphere, round cylinder (transverse to flow and infinite in length), elliptic cylinder, prolate spheroid, oblate spheroid, circular disc (normal to the flow). The velocity function Φ and stream function ψ are determined for each of the quadrics, from these the velocity component formulas are derived.

For the sphere the velocity components that may be used to depict the flow about the sphere are:

$$q_x = (1 - a^3/x^3)q_o; \quad q_y = (1 + a^3/2y^3)q_o; \quad q_t = 1.5 q_o \text{ Sin } \theta$$

where: q_x and q_y velocity components in direction of x and y axes

q_o, velocity of free stream

---

[3] Zahm, A. F., "Flow and Drag Formulas for Simple Quadrics", National Advisory Committee for Aeronautics Annual Report Number 253 of 1926.

q_t, is component tangent to an element of arc ds in direction of flow

a, is the spherical radius

θ, the polar angle

The zonal pressure drag $0.2\pi \int p\, y\, dy$, where a zone is defined as the part of a surface bounded by two planes normal to q_o and on integration

$$D = \pi a^2 \sin^2 \theta \left(1 - \frac{9}{8} \sin^2 \theta\right) 1/2\ \rho\ V_o^2$$

V_o is the free stream velocity

ρ is the mass density in slugs/cu. ft.

$q_o = 1/2\ \rho\ V_o^2$, the dynamic pressure

from this the drag coefficient is computed

$$C_D = \frac{D}{q\ \pi\ a^2}$$

Experiment indicates that there is considerable variation in the drag coefficient with changing Reynold's Number. For Reynolds Number greater than 10000 the sphere drag coefficient of $C_D = 0.50$ is suggested (recent tests indicate values of $C_D = .30$, approximate, for spheres) and from this the drag in pounds is obtained by:

$$D = .5\ q\ \pi\ a^2$$

Since this study is devoted to the three dimensional problem, Zahm's conclusions concerning the round and elliptic cylinders transverse to the flow and infinitely long will be omitted.

The formulas concerning the prolate spheroid are of particular interest. Expressions for the velocity components are as follows:

$$q_x = (1 - n)q_o \quad ; \quad q_y = (1 + m)q_o \quad ; \quad q_t = (1 + K_1)q_o \sin \theta$$

K_1 is Lamb's Inertia factor[4], values of which may be obtained from Figure 4. The terms m, n are values of K_1 based upon the fineness ratio of the confocal ellipse.

Zonal Pressure Drag may be obtained by the following expression:

$$D/q = \pi y^2 - \frac{\pi a^2}{c^2}(1 + K_1)^2 y^2 + \frac{\pi a^2 b^2}{c^4}(1 + K_1)^2 \log \frac{b^4 + c^2 y^2}{b^4}$$

where: y = radius of spheroid at any point along the axis

a = semi-major axis

b = semi-minor axis

c = focal distance

by means of the above expression the distribution along the major axis may be plotted.

The stream and potential function (Φ and ψ) expressions for the prolate spheroid are as follows:

$$\Phi = - (1 + m)\, q_o x \text{ and } \psi = - 1/2\, (1 - n)\, q_o y^2$$

where: $m = a^3/2a'^3$ and $n = a^3/a'^3$

a' is semi-major axis of the confocal ellipse.

These expressions are derived from other expressions in elliptic coordinates that may be found in texts such as Lamb's "Hydrodynamics"[5] and

---

[4] Lamb, Horace, "The Inertia-Coefficients of an Ellipsoid Moving in Fluid", Technical Report of the Advisory Committee for Aeronautics (British) for 1918-1919, Volume 1, page 128.

[5] Ibid., pp. 71, 105, 108

others. Derivation of the above expressions for Φ and ψ are not presented here as they are not used herein, and the formulae are presented merely for purposes of record.

Zahm discusses procedures for constructing the velocity distribiutions about these simple quadrics when the flow is oblique. The procedure in essence is to resolve the stream into component streams, U and V, each having its own velocity at any flow point, as in Figure 1. Combining the individuals gives their resultant, and from this the pressure at the point "p" may be computed. A practical disadvantage of this method is that for every angle of attack to be investigated a different flow pattern must be constructed.

The case of the oblate spheroid is also considered by Zahm, but is of little interest as regards the purpose of this study, that of predicting aerodynamic forces and moments acting on arbitrary bodies of revolution.

Karman[6] presents a procedure for determining theoretically the velocity distribution and hence the pressure distribution on airship hulls. This procedure utilizes sources and sinks of verying strength superimposed on a uniform stream. The sources and sinks are arranged along a line representing the longitudinal axis of the hull. Strength of the sources and sinks are then varied until the resulting flow or streamline pattern has a $\psi = 0$ stream boundary very closely approximating the contour of the hull. From this it is apparent that the

---

[6] Karman, T. von, "Calculations of Pressure Distribution on Airship Hulls", National Advisory Committee for Aeronautics Technical Memorandum 574, July 1930.

procedure will prove to be cumbersome, involving several attempts to arrive at the proper variation of the strength of the sources and sinks. Figure 2. illustrates the variation of source and sink strength along the longitudinal axis. Also, a plot indicating the variation of dynamic pressure, q, from bow to stern is included.

In this paper it is stated that the flow about the bow or forward half of the hull is practically independent of the sinks representing the stern or rear half of the hull. Conversely, the flow at the stern is independent of the forward sources. This permits the computations to be made separately for bow and stern. This treatment of the problem is graphically illustrated by Figure 3.

The two cases of flow considered are, symmetrical or flow parallel to the axis, and unsymmetrical or flow at an angle to the axis. In both cases the simple potential flow is the basis for computing the pressure distribution. For both cases the results are unsatisfactory as regards prediction of aerodynamic forces and moments acting on the hull. In the symmetrical case the resultant pressure distribution will not yield the drag and for the unsymmetrical case only an estimate of the aerodynamic moment may be obtained; and it will also not give the cross wind or normal force. To determine the normal force Karman assumes that the hull is followed by a vortex distribution. This assumption is similar to a familiar treatment of the problem of estimating the normal force or lift of an airfoil by modifying the pressure distribution obtained by potential flow theory through introduction of the concept of circulation.

As mentioned before, the theory is based on the potential flow,

beginning with the expression for the stream and potential function of a simple source:

$$\psi = -\frac{Q}{4\pi\rho} \quad ; \quad \Phi = \frac{Q}{4\pi}(1 + \cos\sigma)$$

where: Φ, the potential function

ψ, the stream function

ρ, the length of the radius vector

σ, the angle between radius vector and the axis of symmetry

Karman then computes the function of flow and velocity components for a line source of length a and yield q per unit length. Then considering a point P located somewhere along the line source where ρ' and ρ'' represent the distance of point P from left and right end of the line source the stream function may be written

$$\psi = -\frac{q}{4\pi}(a + \rho' - \rho'')$$

but the total yield of the line source of length is $Q = qa$ and the stream function for the element of length of a becomes:

$$\psi = -\frac{Q}{4\pi}(1 + \rho' - \rho'')$$

from this the velocity components may be easily derived. Dividing the longitudinal axis up into elemental line sources of length "a" then the expression for the stream function representing the summation of these elemental line sources of varying yield or strength is

$$\Sigma\psi_2 = -\frac{1}{4\pi}\left(1 + \frac{\rho_i' - \rho_i''}{a}\right)Q_i$$

on which the parallel flow must be superposed and which results in

$$\psi = \frac{Ur^2}{2} - \sum_{i=1}^{h} \frac{Qi}{4\pi} \left(1 + \frac{\rho'i - \rho''i}{a}\right)$$

The lines ψ = constant represent streamlines and $\psi = 0$ must yield the axis and the envelope curve. Therefore, putting $\psi = 0$ for just as many points of the envelope curve as there are unknown line sources will result in a system of linear equations for the determination of the required yield Q_i for each source.

The process of developing the system of linear equations and solving them is complex and will involve several trials. The unknown nondimensional quantities are assigned a symbol as follows:

$$\frac{Q_i}{2U\pi a^2} = Z_i$$

Also ρ'_{ik} and ρ''_{ik} denote length of radius vectors leading from end points of the i the line source to the point P forming the coefficient

$$1 + \frac{\rho'_{ik} - \rho''_{ik}}{a} = c_{ik}$$

the quantity r_k denotes the radial distance from the longitudinal axis to the point P. Then the condition $\psi = o$, applied to the "n" line sources and "n" marginal points "p" yield equations:

$$\begin{aligned}
c_{11} z_1 + c_{21} z_2 + \ldots + c_{n1} z_n &= \left(\frac{r_1}{a}\right)^2 \\
\vdots \quad\quad \vdots \quad\quad \vdots \quad\quad &\vdots \\
c_{1n} z_1 + c_{2n} z_2 + \ldots + c_{nn} z_n &= \left(\frac{r_n}{a}\right)^2
\end{aligned}$$

On finally solving these equations each source may be assigned the proper strength or yield and then the velocity distribution field constructed.

In the case of unsymmetrical flow, the procedure is as previously explained[7] and involves consideration of the combined flow first parallel to the longitudinal axis and then transverse to the longitudinal axis. This procedure is illustrated by Figure 1.

The entire procedure is laborious to the extent of becoming useless for practical design development purposes. It must be remembered that the flow pattern for each angle of attack must be determined and also the nature and extent of variation of the flow pattern considered by passing planes diametrically through the hull or body. Finally the results of these pressure distributions must be integrated to yield the transverse force distribution represented by curve b of Figure 3.

Karman best evaluates this method by stating that the modification of the pressure distribution as described previously is necessary to obtain lift and drag by Karman's source and sink procedure. Although Karman states that the modification can be achieved and illustrates the results by curve d of Figure 3, he does not elaborate on the procedure as a whole.

The distribution of normal pressures on a prolate spheroid is the subject of a report by R. Jones[8]. The study reported was motivated by the desire to develop procedures by which airloads might be predicted that would be useful in design of the airship hull structure. Quantitative comparison of theoretically determined pressures, transverse and

---

[7] Cf. ante., p. 8

[8] Jones, R., "The distribution of Normal Pressures on a Prolate Spheroid", Technical Report of the Aeronautical Research Committee (British) for 1926-7, R and M 1061 pg. 516.

longitudinal forces with those obtained by experiment is a feature of this report.

Previous consideration of the problem of flow about a streamlined body with longitudinal axis parallel to the direction of flow proved to be of little value since it was almost impossible to modify the results to take into account oblique flow. For reasons of simplification and to form a foundation for future study this study of the flow about a prolate spheroid is considered.

Figure 5. illustrates the system of axes and notation used in presenting the theory on which Jones[8] paper is based. Some of the symbols and notation used, not illustrated in Figure 5., are described as follows:

O, Center of the spheroid

Ω, Angular velocity of the spheroid about O_z, (Z axis)

ψ, Angle between wind direction and axis O_x, i.e. the angle of yaw for the spheroid

V, the resultant velocity of O tangent to the curve path

u and v, components of velocity along O_x and O_y such that:

$$u = V \operatorname{Cos} \psi \ , \quad v = - V \operatorname{Sin} \psi$$

a and b, represent semi-major and semi-minor axes of the spheroid respectively

$e = \sqrt{1 - b^2/a^2}$, Eccentricity of the spheroid

P, a point on the surface of the spheroid location of which is described in spheroidal coordinates by:

$$x = ae$$
$$y = ae \sqrt{1 - \mu^2} \sqrt{\zeta^2 - 1} \operatorname{Cos} \omega$$
$$z = ae \sqrt{1 - \mu^2} \sqrt{\zeta^2 - 1} \operatorname{Sin} \omega$$

where μ, ζ and ω = constant are quadric surfaces confocal with the spheroid under consideration.

The velocity potential for the prolate spheroid is obtained from Lamb's "Hydrodynamics"[9]

$$\phi = \phi_1 + \phi_2 + \phi_3$$

where values of ϕ_1, ϕ_2, and ϕ_3 are as follows:

$$\phi_1 = \frac{a u}{\frac{1}{1-e^2} - \frac{1}{2e}\log\frac{1+e}{1-e}} \mu \left\{ \frac{1}{2}\zeta \log\frac{\zeta+1}{\zeta-1} - 1 \right\}$$

$$\phi_2 = \frac{-aev}{\frac{1}{2}\log\frac{1+e}{1-e} - \frac{e-2e^3}{1-e^2}} \sqrt{1-\mu^2}\,\sqrt{\zeta^2-1}$$

$$\phi_3 = A\mu \sqrt{1-\mu^2}\,\sqrt{\zeta^2-1} \left\{ \frac{1}{2}\log\frac{\zeta+1}{\zeta-1} - \frac{\zeta}{\zeta^2-1} \right\} \cos\omega$$

$$\left\{ \frac{3}{2}\log\frac{\zeta+1}{\zeta-1} - 3 - \frac{1}{\zeta^2-1} \right\} \cos\omega$$

where $$A = \frac{(b^2 - a^2)\,\Omega}{\frac{3}{2}\left(\frac{2}{e^2} - 1\right)\log\frac{1+e}{1-e} - \frac{6}{e} + \frac{e}{1-e^2}}$$

From this it follows that the pressure "p" at any point is given by

$$p/\rho = \frac{\partial \phi}{\partial t} - \frac{1}{2} q^2$$

$$q^2 = \left(\frac{\partial \phi}{\partial \mu} \cdot \frac{\partial \mu}{\partial S_\mu} \right)^2 + \text{two similar terms}$$

[9] Lamb, Horace, "Hydrodynamics", 3rd Edition pgs. 103 to 106.

where ∂S_μ is a line element on the intersection of the surfaces ζ = constant and ω = constant, ϕ is the potential function.

$$\frac{\partial \mu}{\partial S_\mu} = \frac{1}{ae}\sqrt{\frac{1-\mu^2}{\zeta^2-\mu^2}} \quad , \quad \frac{\partial \zeta}{\partial S_\zeta} = \frac{1}{ae}\sqrt{\frac{\zeta^2-1}{\zeta^2-\mu^2}}$$

$$\frac{\partial \omega}{\partial S_\omega} = \frac{1}{ae}\,\frac{1}{\sqrt{(1-\mu^2)(\zeta^2-1)}}$$

However, since $\partial\phi/\partial t$ expresses the rate at which ϕ is increasing at a fixed point in space, where as the value of ϕ here is referred to an origin which is in motion and the expression then becomes

$$\frac{\partial \phi}{\partial t} = -\left(\frac{\partial \phi}{\partial \mu}\cdot\frac{\partial \mu}{\partial S_\mu}\cdot\frac{dS_\mu}{dt}\right) - \left(\frac{\partial \phi}{\partial \zeta}\cdot\frac{\partial \zeta}{\partial S_\zeta}\cdot\frac{dS_\zeta}{dt}\right) - \left(\frac{\partial \phi}{\partial \omega}\cdot\frac{\partial \omega}{\partial S_\omega}\cdot\frac{dS_\omega}{dt}\right)$$

the terms:

$$\frac{dS_\mu}{dt} = l_1(u - y\Omega) + l_2(v + x\Omega)$$

$$\frac{dS_\zeta}{dt} = m_1(u - y\Omega) + m_2(v + x\Omega)$$

$$\frac{dS_\omega}{dt} = n_1(u - y\Omega) + n_2(v + x\Omega)$$

where l_1, m_1, n_1, l_2, m_2, n_2 are direction cosines of O_x and O_y. Considering the equation of the spheroid.

$$\zeta = \text{constant} = \frac{1}{e} \quad \text{and} \quad \frac{x^2}{a^2} + \frac{y^2+z^2}{b^2} = 1$$

the direction cosines of the normals to the surface at the point

$$l_1 = a \sin\epsilon / \sqrt{a^2 \sin^2\epsilon + b^2 \cos^2\epsilon}$$

$$m_1 = b \cos\epsilon / \sqrt{a^2 \sin^2\epsilon + b^2 \cos^2\epsilon}$$

$$n_1 = 0$$

and $$l_2 = -b \cos\epsilon \cos\omega / \sqrt{a^2 \sin^2\epsilon + b^2 \cos^2\epsilon}$$

$$m_2 = a \sin\epsilon \cos\omega / \sqrt{a^2 \sin^2\epsilon + b^2 \cos^2\epsilon}$$

$$n_2 = -\sin\omega$$

On the surface of the prolate spheroid,

$$\frac{d\xi_\mu}{dt} = \frac{a u \sin\epsilon - b v \cos\epsilon \cos\omega - ab\Omega \cos\omega}{\sqrt{a^2 \sin^2\epsilon + b^2 \cos^2\epsilon}}$$

$$\frac{d\xi_\zeta}{dt} = \frac{b u \cos\epsilon + a v \sin\epsilon \cos\omega + (a^2 - b^2)\Omega \sin\epsilon \cos\epsilon \cos\omega}{\sqrt{a^2 \sin^2\epsilon + b^2 \cos^2\epsilon}}$$

$$\frac{d\xi_\omega}{dt} = -\sin\omega (v + a\Omega \cos\epsilon)$$

Let $$\frac{\frac{1}{2e}\log\frac{1+e}{1-e} - 1}{\frac{1}{2e}\log\frac{1+e}{1-e} - \frac{1}{1-e^2}} = -L$$

$$\frac{\frac{1}{2e}\log\frac{1+e}{1-e} - \frac{e}{1-e^2}}{\frac{1}{2}\log\frac{1+e}{1-e} - \frac{e - 2e^3}{1-e^2}} = -M$$

and $$\frac{\frac{3}{2e}\log\frac{1+e}{1-e} - 3 - \frac{e^2}{1-e^2}}{\frac{3}{2}\frac{2-e^2}{e}\log\frac{1+e}{1-e} - 6 + \frac{e^2}{1-e^2}} = -N$$

then with appropriate substitutions

$$\frac{\partial\phi}{\partial\mu}\cdot\frac{\partial\mu}{\partial S_\mu} = \frac{1}{\sqrt{a^2\sin^2\epsilon + b^2\cos^2\epsilon}}$$
$$\left\{ a u L \sin\epsilon - b v M \cos\epsilon\cos\omega - \frac{b}{a}(a^2-b^2)\Omega N\cos 2\epsilon\cos\omega \right\}$$

$$\frac{\partial\phi}{\partial\zeta}\cdot\frac{\partial\zeta}{\partial S_\zeta} = \frac{1}{\sqrt{a^2\sin^2\epsilon + b^2\cos^2\epsilon}}$$
$$[b u\cos\epsilon + a v\sin\epsilon\cos\omega + (a^2-b^2)\Omega\sin\epsilon\cos\epsilon\cos\omega]$$

$$\frac{\partial\phi}{\partial\omega}\cdot\frac{\partial\omega}{\partial S_\mu} = -\sin^2\omega\left\{ v M + \frac{a^2-b^2}{a}\Omega N\cos\epsilon \right\}$$

After reduction and on substituting for the velocity components u and v the following expression is obtained;

$$p = a_0 + a_1\cos\omega + a_2\cos\omega^2 + a_3\sin^2\omega + (b_1\cos\omega + b_2\cos^2\omega + b_3\sin^2\omega)\Omega + (c_2\cos^2\omega + c_3\sin^2\omega)\Omega^2$$

where:

$$a_0 = \frac{1}{2}\rho V^2 \cos^2\psi \left\{ 1 - \frac{(1+L)^2 \sin^2\epsilon}{\sin^2\epsilon + (b^2/a^2)\cos^2\epsilon} \right\}$$

$$a_1 = -\frac{1}{2}\rho V^2 \frac{2(b/a)(1+L)(1+M)\sin\psi\cos\psi\sin\epsilon\cos\epsilon}{\sin^2\epsilon + (b^2/a^2)\cos^2\epsilon}$$

$$a_2 = \frac{1}{2}\rho V^2 \sin^2\psi \left\{ 1 - \frac{(b^2/a^2)(1+M)^2\cos^2\epsilon}{\sin^2\epsilon + (b^2/a^2)\cos^2\epsilon} \right\}$$

$$a_3 = \frac{1}{2}\rho V^2 \sin^2\psi \left\{ 1 - (1+M)^2 \right\}$$

$$\frac{1}{2} b_1 \Omega = \frac{\rho V^2 b}{2R} \cos\psi \sin\epsilon \left\{ \frac{(1+L)(1+e^2N\cos 2\epsilon}{\sin^2\epsilon + (b^2/a^2)\cos^2\epsilon} - 1 \right\}$$

$$\frac{1}{2} b_2 \Omega = \frac{\rho V^2 a}{2R} \sin\psi \cos\epsilon \left\{ \frac{(b^2/a^2)(1+M)(1+e^2N\cos 2\epsilon}{\sin^2\epsilon + (b^2/a^2)\cos^2\epsilon} - 1 \right\}$$

$$\frac{1}{2} b_3 \Omega = \frac{\rho V^2 a}{2R} \sin\psi\cos\epsilon \left\{ (1+M)(1+e^2N) - 1 \right\}$$

$$c_2 \Omega^2 = \frac{a^2\rho V^2}{2R^2} \left\{ \cos^2\epsilon + \frac{b^2}{a^2}\sin^2\epsilon - \frac{(b^2/a^2)(1+e^2N\cos 2\epsilon)^2}{\sin^2\epsilon + (b^2/a^2)\cos^2\epsilon} \right\}$$

$$c_3 \Omega^2 = \frac{a^2\rho V^2}{2R^2} \cos^2\psi \left\{ 1 - (1+e^2N)^2 \right\}$$

where R is the radius of the circle in which O moves, i.e., $V = R\Omega$.

Substituting u for $V\cos\psi$, v for $-V\sin\psi$, and Ω for V/R the terms independent of $(1 + L)$, $(1 + M)$, $(1 + e^2N \cos^2\epsilon)$ and $(1 + e^2N)$, reduced to

$$\frac{1}{2}\rho(u - y\Omega)^2 + \frac{1}{2}\rho(v + x\Omega)^2$$

or $\frac{1}{2}\rho$ X (resultant velocity)^2 at the point whose co-ordinates are x and y.

Hence, putting U for the resultant velocity, then

$$\frac{p}{\rho} = \frac{1}{2}U^2$$

$$-\frac{1}{2}V^2\left\{\frac{(1+L)\sin\epsilon\cos\psi+(b/a)(1+M)\cos\epsilon\sin\psi\cos\omega}{\sqrt{\sin^2\epsilon+(b^2/a^2)\cos^2\epsilon}}\right\}^2$$

$$+\frac{V^2}{R^2}\cdot\frac{b(1+e^2N\cos 2\epsilon)}{\sin^2\epsilon+(b^2/a^2)\cos^2\epsilon}$$

$$\times\left\{(1+L)\sin\epsilon\cos\psi+(b/a)(1+M)\cos\epsilon\sin\psi\cos\omega\right\}\cos\omega$$

$$-\frac{1}{2}V^2/R^2\cdot\frac{b^2(1+e^2N\cos 2\epsilon)^2}{\sin^2\epsilon+(b^2/a^2)\cos^2\epsilon}\cos^2\omega-\frac{1}{2}V^2\sin^2\psi\sin^2\omega(1+M)^2$$

$$+\frac{V^2}{R^2}\cdot\frac{b(1+e^2N\cos 2\epsilon)}{\sin^2\epsilon+(b^2/a^2)\cos^2\epsilon}$$

$$-\frac{1}{2}\frac{V^2}{R^2}a^2\cos^2\epsilon\sin^2\omega(1+e^2N)^2$$

$$=\frac{1}{2}U^2-\frac{V^2}{2}\left\{\frac{a(1+L)\sin\epsilon\cos\psi}{\sqrt{a^2\sin^2\epsilon+b^2\cos^2\epsilon}}\right.$$

$$\left.+\frac{b(1+M)\cos\epsilon\sin\psi\cos\omega-(ba/R)(1+e^2N\cos 2\epsilon)\cos\omega}{\sqrt{a^2\sin^2\epsilon+b^2\cos^2\epsilon}}\right\}$$

$$-\frac{V^2}{2}\sin^2\omega\left\{(1+M)\sin\psi-(a/R)\cos\epsilon(1+e^2N)\right\}^2$$

$$=\frac{1}{2}U^2-\frac{1}{2}\left\{\left(\frac{\partial\phi}{\partial s_\mu}\right)^2+\left(\frac{\partial\phi}{\partial s_\omega}\right)^2\right\}$$

with $1+L$, $1+M$, $1+e^2N\cos 2\epsilon$ and $1+e^2N$ substituted for L, M, $e^2N\cos 2\epsilon$ and e^2N respectively.

Of primary interest is the case when $\Omega = 0$ the expression could have been derived more simply by supposing the body reduced to rest by imposing the velocity components u and v on the entire system. It would then be necessary to add the terms ux and vy respectively to the expression for ϕ_1 and ϕ_2 . The added terms are $uae\mu\xi$ and $vae\sqrt{1-\mu^2}\sqrt{\xi^2-1}\cos\omega$ Therefore,

$$p/\tfrac{1}{2}\rho V^2 = 1 - q^2, \text{ where } q^2 = \left(\frac{\partial\phi'}{\partial\xi_\mu}\right)^2 + \left(\frac{\partial\phi'}{\partial\xi_\omega}\right)^2$$

ϕ' the new value of ϕ. $\frac{\partial\phi'}{\partial\xi_\xi} = 0$. This results in the expression,

$$1 - \frac{p}{\frac{1}{2}\rho V^2} = \frac{1}{V^2(a^2\sin^2\epsilon + b^2\cos^2\epsilon)} \times \left[au(1+L)\sin\epsilon - bv(1+M)\cos\epsilon\cos\omega\right]^2 + v^2(1+M)^2\sin^2\omega$$

It is obvious that q = 0 when $\omega = 0$ and $\tan\epsilon = \frac{bv(1+M)}{au(1+L)}$

Let P_o be the point at which this occurs, and let η be the inclination of the normal at this point to Ox, and ϵ_o be the value of ϵ at this point.

Then

$$\tan\eta = \frac{a}{b}\tan\epsilon_o = \frac{v}{u}\cdot\frac{1+M}{1+L}$$

The maximum value of q^2 on the prolate spheroid is

$$u^2(1+L)^2 + v^2(1+M)^2 = Q^2.$$

If θ be the inclination of the normal at the point P, whose eccentric angle is ϵ , to the axis Ox, $\tan\theta = (a/b)\tan\epsilon$.

This permits writing the expression for $1 - p/\frac{1}{2}\rho V^2$ in the form

$$1 - \frac{p}{\frac{1}{2}\rho V^2} = \frac{u^2(1+L)^2 + v^2(1+M)^2}{V^2} - \frac{\{bu(1+L)\cos\epsilon + av(1+M)\sin\epsilon\cos\omega\}^2}{V^2(a^2\sin^2\epsilon + b^2\cos^2\epsilon)}$$

$$= \frac{Q^2}{V} - \frac{Q^2}{V^2}\{\cos\theta\cos\eta + \sin\theta\sin\eta\cos\omega\}^2$$

The average pressure at any section $x = x_0$ of the prolate spheroid through the point P is

$$P' = \frac{1}{2\pi}\int_0^{2\pi} p \cdot d\omega$$

The part independent of Ω may be written down directly from the expression for $1 - \frac{p}{\frac{1}{2}\rho V^2}$ as above

$$\frac{P'}{\frac{1}{2}\rho V^2} = 1 - \frac{Q^2}{V^2} + \frac{Q^2}{V^2}\left(\cos^2\theta\cos^2\eta + \frac{1}{2}\sin^2\theta\sin^2\eta\right)$$

The part containing V^2/R is

$$\frac{P_1'}{\frac{1}{2}\rho V^2} = \frac{a}{R}\sin\psi\cos\epsilon\left\{\frac{b^2(1+M)(1+e^2N\cos 2\epsilon)}{a^2\sin^2\epsilon + b^2\cos^2\epsilon} - 2 + (1+M)(1+e^2N)\right\}$$

and finally the part containing V^2/R^2

$$\frac{P_2'}{\frac{1}{2}\rho V^2} = \frac{1}{2}\frac{a^2}{R^2}\left\{\cos^2\epsilon + \frac{b^2}{a^2}\sin^2\epsilon + \cos^2\epsilon - \frac{b^2(1+e^2N\cos 2\epsilon)^2}{a^2\sin^2\epsilon + b^2\cos^2\epsilon} - (1+e^2N)^2\right\}$$

$$P' = P'_1 + P'_2 + P'_3.$$

The longitudinal force, i.e., the force along the major axis, is

$$\int_{s_1}^{s_2}\int_0^{2\pi} p \cdot d\omega \cdot r\cos\theta \cdot ds$$

where ds is an element of length along a section through the major axis ($s = 0$ in the plane xOy) and s_1, s_2, respectively, are values of s at

the forward and after-end of the spheroid. r is the radius of the section through P perpendicular to the major axis and

$$\cos\theta = dr/ds.$$

Then the longitudinal force is obtained by :

$$X = \int_{O_1}^{O_2}\int_{0}^{2\pi} p \cdot d\omega \cdot r dr = 1/2 \int_{O_1}^{O_2}\int_{0}^{2\pi} p \cdot d\omega \cdot dr^2$$

O_1, O_2 = r AT ENDS OF MAJOR AXIS.

The component of the pressure p in the plane x0y is $p \cos\omega$. The resultant pressure on the section perpendicular to xoy, through a point whose eccentric angle is ϵ, is

$$P'' = b \sin\epsilon \int_0^{2\pi} p \cos\omega \, d\omega,$$

acting normal to the generator in the plane of xy

$$P'' = b \sin\epsilon \int_{-1}^{+1} p \cdot d(\sin\omega) = \int_{-z_0}^{+z_0} p \cdot dz$$

z_0 is the radius of the section ($= b \sin\epsilon$).

The resultant lateral force is obtained by

$$= \int_{s_1}^{s_2} P'' \sin \quad \cdot ds$$

$$= \int_{x_1}^{x_2} P'' \cdot dx$$

The yawing moment about the axis of z is $\int P'' \ell \cdot ds$, where ℓ is the perpendicular distance between the z axis and the line of action of P'' or the normal at the point ϵ in the plane x0y.

$$\ell = \frac{(a^2-b^2)\sin\epsilon\cos\epsilon}{\sqrt{a^2\sin^2\epsilon + b^2\cos^2\epsilon}}, \quad \frac{ds}{d\epsilon} = \frac{\sqrt{dx^2+dy^2}}{d\epsilon}$$

$$= \sqrt{a^2\sin^2\epsilon + b^2\cos^2\epsilon}$$

therefore the yawing moment is

$$\int P'' (a^2 - b^2) \sin\epsilon \cos\epsilon \cdot d\epsilon$$

$$= -\int P'' a^2 \cos\epsilon \, d(\cos\epsilon) - \int P'' b^2 \sin\epsilon \, d(\sin\epsilon)$$

$$= -1/2 \int P'' d(x^2 + y^2)$$

To facilitate structural design of airship hulls, Upson and Klickoff[10] have utilized the theory developed by Jones[11] concerning the theoretical computation of pressures, transverse and longitudinal force distributions for a prolate spheroid. The expressions of Jones are further reduced and simplified to facilitate application of the spheroidal formulas to the semi-spheroidal airship shapes. Study of this report indicated good possibilities for application of formulas and procedure to other bodies than airship hulls differing both in shape and magnitude.

Upson and Klickoff here suggest the idea that for an arbitrary body of revolution of irregular or even bluff shape an equivalent spheroidal shape having the same apparent mass properties may be chosen. Several other procedures are suggested, example of which is breaking the body up into increments of length and determining equivalent spheroids for each increment, thus computing the transverse and longitudinal forces per unit length and finally summing up these forces for each increment to determine both distribution and magnitude of the net forces.

The procedures of Upson and Klickoff are not modified to take into account the differences of the theoretical distributions when compared with the experimental. Reason for this is that their prime purpose was facilitating structural analysis and they were interested in a conservative estimate of the distribution over the hull length and not in the question as to the magnitude of the cross wind force or longitudinal force in direction of the X axis.

---

[10] Upson, R. H. and Klickoff, W. A., "Application of Practical Hydrodynamics to Airship Design", National Advisory Committee for Aeronautics Technical Report 405 dated 1931.

[11] Jones, R., op. cit., p. 516.

Notation and symbols used are illustrated by Figure 5., which was previously referenced in connection with Jones[12] derivations for the prolate spheroid. Although many of the symbols and notations are common to both papers, Upson and Klickoff have simplified the formulas by introduction of the tangent, sine and cosine functions of α. the angle between the longitudinal or X axis, and the tangent to the hull contour at any point "P". In the Jones treatment it was necessary to define the normals to the surface at the point.

In essence the work of Upson and Klickoff may be reduced to a consideration of three expressions. These consist of an expression for the incremental transverse force per unit length of hull, incremental longitudinal force (parallel to the X axis), and an expression for computing the moment. The expressions are derived from the previous work of Jones[12].

In pitched flight, where the angle of the relative wind with the longitudinal axis is denoted by θ and the radius of curvature $R = \infty$, the expression for the incremental transverse force per unit length is;

$$\Delta F_t = q \frac{AB}{2} \frac{ds}{dx} \text{Cos}^2 \alpha \text{ Sin2 } \theta = q \frac{AB}{2} \pi r \text{ Sin2 } \alpha \text{ Sin2 } \theta$$

where $A = 1 + K_1$

$B = 1 + K_2$

K_1 and K_2 are Lamb's Inertia Coefficients for prolate spheroids (See Figure 4.)

r = y ordinate or radius of spheroid at point "P".

and other symbols are as shown in Figure 5.

---

[12] Cf. ante., pp. 21 and 22.

Similarly for the case of pitched straight flight the expression for the longitudinal component of force per unit length of hull is

$$\Delta F_L = q\left[2 - 2A^2\,\mathrm{Cos}^2\alpha\mathrm{Cos}^2\theta - B^2\,(1 + \mathrm{Sin}^2\alpha)\,\mathrm{Sin}^2\theta\right]\pi r\tan\alpha$$

Regarding this component of force, the comment is offered that in the case of airships at low speeds this may be neglected. However, it is warned that the force may not be negligible at high speeds.

An expression for determining the moment about the center of volume of the prolate spheroid is presented. This, too, was derived from the work of Jones[13] and Upson and Klickoff have simply reduced the expression, simplifying it to the barest elements. The expression is

$$M_o = q(K_2 - K_1)\,(\mathrm{vol})\,\mathrm{Sin}2\theta.$$

Some comparison of theoretical transverse force distributions with experimental distribution is presented. Several familiar airship hulls constitute the illustrative example. There is no further discussion of the longitudinal force distribution. Apparently friction drag of airships is sufficiently great to permit computation of the pressure drag or effect of the summation of incremental longitudinal forces as a proportion of the skin friction drag. The section devoted to drag computation discusses primarily determination of the magnitude of resistance due to skin friction.

---

[13] Cf. ante., pp. 21 and 22

DEVELOPEMENT OF THE PROCEDURE

Prediction of Normal Force.

Integration of experimentally obtained transverse force distribution curves for prolate spheroids results in a net or resultant total transverse force. It is at once recognized that this net transverse force is the normal or cross wind aerodynamic force acting on the body. Representative of such experimentally obtained transverse force distributions are the curves of Figure 6., which record test results obtained by a model prolate spheroid of L/D = 4.0, length, two feet, in a stream of forty feet per second velocity.

The theoretical transverse force distribution for the prolate spheroid may be constructed by use of the formula for ΔF_t[14]. A study of experimental transverse force data, figure 6., has revealed a pattern that may be used to modify the theoretical transverse force distributions to render the resultant distribution consistent with those determined by experiment.

A study of the formula for the incremental transverse force per unit length of hull

$$\Delta F_t = q \pi \frac{AB}{2} y \operatorname{Sin2} \alpha \operatorname{Sin2} \theta$$

$$r = y \text{ at the point "P"}$$

indicates that the only variable terms, that are functions of fineness ratio, are included in the following:

$$\pi \frac{AB}{2} y \operatorname{Sin2} \alpha$$

---

[14] Cf. ante., pp. 24

and by dividing the spheroid up into increments of length and plotting the variation of this function with length, then the basic pattern for the transverse force distribution may be obtained. Tables I through VIII of Appendix A are required to compute the variations of y Sin2 α for prolate spheroids of fineness ratios 2, 3, 4, 4.5, 5, 7 and 10. Table IX represents average or mean values obtained by comparing theoretical transverse force distributions with experimentally obtained distributions[15] such as Figure 6. By means of Table IX the Experimental Correction Factors are obtained, and when coupled with the results of Table I through VIII corrected distributions of y Sin2 α for the prolate spheroids having fineness ratio or L/D values of 2, 3, 4, 4.5, 5, 7 and 10 are obtained. A comparative plot of these distributions is found in Figure 7. Mechanical integration of the area under these curves results in the net values of $\sum$ y Sin2 α for each fineness ratio. These values are multiplied by factors, including Lamb's Inertia Coefficients, and the resultant values of $\pi \frac{AB}{2}$ y Sin2 α computed in Table XI is plotted in Figure 8. The normal force is then obtained by

$$N = q \pi \frac{AB}{2} \sum y \text{ Sin2 } \alpha \text{ Sin2 } \theta$$

However, on applying these results to the case of the two foot long prolate spheroid of fineness ratio four in a forty foot per second stream (the experimental force test results may be found in the report by Jones[16]), it is found that an additional correction factor, here

---

[15] Jones, R., op. cit., p. 535, Figure 8.

[16] Jones, R., loc. cit.

termed the Angle of Attack Correction Factor K_θ, is necessary to give agreement between predicted and measured results. Table XII illustrates the type or nature of the correction required and the factor K_θ thus computed will be used in connection with the procedure set forth here. Variation of the Angle of Attack Correction Factor K_θ is plotted on Figure 9. Finally, the normal force acting on any prolate spheroid of given fineness ratio may be predicted by

$$N = q \pi \frac{AB}{2} \Sigma y \, \mathrm{Sin2}\, \alpha \, \mathrm{Sin2}\, \theta \, K_\theta$$

In the case of any bluff body of revolution, say a semi-cylindrical shape, it is necessary to choose an equivalent prolate spheroid having the same inertia coefficients or apparent mass characteristics. Figure 11. illustrates the comparison of the Lamb type inertia coefficients for a cylinder with hemispherical ends with those for the prolate spheroid. On choosing the equivalent spheroid then the normal force may be predicted by use of the above equation.

Prediction of Moment.

Prediction of the moment is best accomplished by use of the formula for yawing moment computation for the prolate spheroid developed and simplified by Jones[17]. Upson and Klickoff[18] also utilize this same formula, which in simplest form is

$$M_o = q(K_2 - K_1) \, \mathrm{Vol.} \, \mathrm{Sin2}\, \theta$$

---

[17] Jones, R., op. cit., p. 556.

[18] Upson and Klickoff, op. cit., p. 7.

where M_o is moment about minor axis of the prolate spheroid

K_1 and K_2 are Lamb's Inertia Factors

Volume, cubic feet

θ, angle of attack or pitch, angle of major axis with the relative wind

In the case of bodies having shape other than that of the prolate spheroid an equivalent spheroid shall be chosen having the identical inertia coefficients or apparent mass characteristics of the body to be tested.

It will be found that in general moments computed by this formula are slightly greater than the moment measured during wind tunnel tests. The formula was applied to a spheroid with L/D = 4.0, that was tested by Jones[19] in a 40 foot per second stream.

For $L/D = 4.0$, $K_1 = .082$, Figure 4.

$K_2 = .860$, Figure 4.

$K_2 - K_1 = .778$

Volume of Spheroid $= 4/3\ \pi ab^2$

$= 4/3\ \pi \times 1.0 \times (.25)^2$

$= .2620$ cu. ft.

at 40 ft./sec. $q = 1/2\ V^2 = .001178 \times (40)^2$

$= 1.902$

$M_o = q\ (K_2 - K_1)$ Volume $\sin 2\theta$

$= 1.902 \times .778 \times .2620 \sin 2\theta = .387 \sin 2\theta$

---

[19] Jones, R., op. cit., p. 536

The moment about the center of volume computed by this formula is compared in Table XIII with those measured by Jones[20] in the wind tunnel. It is noticed that the moment computed by the formula is only eight percent higher than that determined by experiment in the low or useful angle of attack range. This comparison is considered excellent and proves the formula worthwhile for practical use.

Prediction of Drag.

The resistance of bodies of revolution in air has long been a subject of study by students of hydro and aero-mechanics. The airship stimulated study of round bodies such as spheres, ellipsoids, and streamlined shapes. Determination of parasite resistance and its obviously important effect on airplane performance resulted in a study of the resistance of the bluff bodies, cylindrical in shape, which constituted the form of engine nacelles and other protuberences on the airplane. It is dissappointing that very little information exists to show the variation of drag or resistance of bodies of revolution with changes in angle of attack.

Various authorities such as A. C. Charters[21], the ballistician, have suggested separation of body resistance into two parts, that due to pressure or form drag and a part representing skin friction. It logically follows that variation of drag with angle of attack or pitch is a

---

[20] loc. cit.

[21] Charters, A. C., "Some Ballistic Contributions to Aerodynamics", The Journal of Aeronautical Sciences, Vol. 14, Number 3, March 1947. p. 160.

function of the form drag increment alone. Corrections to account for effect of angle of attack would be applied to form drag increment only.

To predict the coefficients of drag or resistance for any body of revolution, particularly a bluff body, it is first necessary to locate some resistance data pertinent to a closely similar shape, i.e., airship hull shapes may be approximated by spheroidal shapes of certain fineness ratio, and cylinders having their axis parallel to the flow. Similar data and coefficients pertinent to other shapes may be found in the Prandtl-Tietjen[22] book. The data discussed here will be in the form of total resistance coefficients. It will then be necessary to divide this into two parts one representing resistance due to skin friction and the other form drag.

Friction drag is found to be a function of Reynold's Number, and von Mises[23] discusses this thoroughly suggesting a formula developed by von Karman

$$C_{Df} = \frac{.072}{\sqrt[5]{R.N.}}$$, where R. N. = Reynold's Number

After computing the coefficient then the drag due to skin friction is computed by:

$$D_f = q\ C_{Df}\ A$$

where A represents the wetted area of the body surface.

---

[22] Prandtl-Tietjens, "Applied Hydro and Aeromechanics", p. 100

[23] Mises, R. von, Theory of Flight. New York: McGraw Hill Book Company, Inc., 1945. p. 98.

As stated before, the coefficients of resistance or drag found in the literature for various bodies of revolution are for the condition of zero angle of attack. On subtracting the skin friction drag from the total drag, the result represents the magnitude of the form drag. Form drag coefficients are computed by:

$$C_{Dp} = \frac{D_p}{q\, A_{po}}$$

where A_{po} is the cross sectional area of the body at its maximum diameter. It seems logical to expect that the increase in form drag D_p as angle of attack is varied is of the order of the increase in projected frontal area of the body on a plane perpendicular to the longitudinal axis when the body is at zero angle of attack. Thus the form drag for any angle of attack θ, may be computed by:

$$D_p = D_{po} \frac{A_p}{A_{po}}$$

where A_p is the projected frontal area of the body for that angle of attack. Finally the total drag of the body for any angle of attack may be predicted by the combination of

$$D = D_p + D_f$$

and by means of this value of the total drag or resistance of the body a coefficient may be computed.

In the cases of bluff bodies it is found by study of data contained in books such as von Mises[24] that the coefficient C_p representing

---

[24] Ibid., p. 98.

form drag of a cylinder when flow is in the direction of the axis has a value of .8 to .9 rather than C_p = 1.11 for a disc or circular plate normal to the flow.

Demonstration of Procedure

A cylindrical body of revolution, Figure 10, was recently tested at 100 miles per hour in the nine foot wind tunnel. Curves of coefficients of lift, drag, and moment, results of this test are presented in Figure 13. These are transformed by Table XIV into coefficients perpendicular and parallel to the longitudinal axis and the moment coefficient transferred to the half length point. Values of Table XIV are plotted on Figure XIV. This body of revolution, considered to be an extreme as far as bluff bodies are concerned, will be used to demonstrate the procedure suggested herein.

It is first necessary to choose an equivalent prolate spheroid having the same inertia coefficients. The ratio of Length/Diameter of the body illustrated in Figure 10.

$$\frac{L}{D} = \frac{35.14}{9.18} = 3.82$$

Refer to Figure 11., which shows a comparison of inertia coefficients of a cylindrical body with those for the prolate spheroids. It is found that an equivalent prolate spheroid of L/D = 2.4 has the same apparent mass characteristics as the body of revolution tested by L/D = 3.82. The normal force[25], or cross wind force may be computed by

$$N = q \pi \frac{AB}{2} \sum y \, \mathrm{Sin2}\, \alpha \, \mathrm{Sin2}\, \theta \, K_\theta$$

---

[25] Cf. ante., p. 28

The variation of $\pi \frac{AB}{2} \Sigma$ y Sin2 α for prolate spheroids of various fineness ratio is contained in Figure 8. For L/D = 2.4

$$\pi \frac{AB}{2} \Sigma \text{ y Sin2 } \alpha = .1725a^2$$

Expressing the normal force in coefficient form

$$C_N = \frac{N}{q\ A}$$

where at 100 mph, $q = 1/2\ \rho\ V^2 = .001178\ (147)^2 = 25.58$

$$A = \frac{\pi\ D^2}{4} = \frac{\pi(.765)^2}{4} = .460 \text{ sq. ft.}$$

and length of body $L/2 = a = 1.462$ ft.

therefore $C_N = \frac{q\ .1725(1.462)^2 \text{ Sin2 } \alpha\ K_\theta}{q \times .46} = \frac{.1725(1.462)^2 \text{ Sin2 } \theta\ K_\theta}{.46}$

$$= .796 \text{ Sin2 } \theta\ K_\theta$$

Values of the predicted normal force coefficient are computed in Table XV for several angles of attack or pitch, θ. These results are then plotted on Figure 14. to illustrate the rather close agreement of test results with predicted results.

As stated previously[26] prediction of the moment is best accomplished by use of the formula

$$M_o = q\ (K_2 - K_1)\ \text{Volume Sin2 } \theta$$

The equivalent spheroid having the same apparent mass characteristics as

---

[26] Cf. ante., p. 28.

the body was previously found to have L/D = 2.4. From Figure 4. the inertia coefficients are found to be

$$K_1 = .169$$

$$K_2 = .746$$

$$K_2 - K_1 = .577$$

The volume of the body tested has been computed to be 1875 cu. in. or 1.085 cu. ft. Also for 100 miles per hour q = 25.58 lbs./sq. ft.

$$M_o = 25.58\ (.577)\ (1.085)\ \text{Sin2}\ \theta = 16.01\ \text{Sin2}\ \theta$$

$$C_{Mo} = \frac{M_o}{qLA} = \frac{16.01\ \text{Sin2}\ \theta}{25.58 \times 2.975 \times .46} = .4575\ \text{Sin2}\ \theta$$

Values of C_{Mo} are computed in Table XV and plotted on Figure 14. Study of the figure, which compares the predicted coefficients with those experimentally determined indicates considerably higher values for the predicted coefficients. However, there is some question regarding the accuracy of the moment coefficients obtained by test. It is to be noticed however, that the slope of the curve of predicted moment coefficients is equal to the slope of the experimentally determined curve. Since the degree of static stability is a function of the slope of the moment coefficient curve this part of the procedure may be relied upon to give some measure of the stability that may be expected.

For prediction of the drag of the body of revolution tested in the wind tunnel a total drag coefficient of $C_D = .845$ for L/D = 3.82 was obtained from data of von Mises[27] for cylinders with axis parallel to the flow.

---

[27] Mises, R. von, op. cit., p. 98.

As stated in the description of the procedure[28] an estimate of the skin friction drag constitutes the first step. The wetted area of the model was computed by means of the dimensions indicated on Figure 10. and found to be 6.1 square feet. The friction drag is computed by the following formula and is a function of the Reynolds Number.

$$C_{Df} = \frac{.072}{\sqrt[5]{R.N.}}$$

In computing Reynold's Number length in feet is the appropriate reference dimension

$$R.N. = \frac{V\ell}{\nu} = \frac{147 \times 2.975}{.000157} = 2.784 \times 10^6$$

and $$\sqrt[5]{R.N.} = \sqrt[5]{2.784 \times 10} = 19.44$$

$$C_{Df} = \frac{.072}{19.44} = .00370$$

By means of this coefficient the drag or skin friction of the wetted area in pounds is computed to be:

$$D_f = q \times C_{Df} \times A = 25.58 \times .0037 \times 6.1 = .4215 \text{ lbs.}$$

The estimated total drag coefficient for model with $\theta = 0^\circ$, $C_D = .845$ will yield an estimated total drag in pounds of

$$D = C_D \times q \times A = .845 \times 25.58 \times .460 = 9.930 \text{ lbs.}$$

From these values the part of the total drag representing the longitudinal components of the pressure on the surface of the body is

---

[28] Cf. ante., p. 33.

$$D_{po} = D - D_f = 9.930 - .4215 = 9.5085 \text{ lbs.}$$

It was explained in the description of the procedure[29] that this quantity varies with changes of angle of attack and that the correction factor is the ratio of the projected frontal area of body A_p when an angle θ to the relative wind, as compared to the projected frontal area when $\theta = 0^o$. Variation of the projected frontal area with angle of attack is indicated in Table XVI.

The total drag of the body for any angle of attack may be predicted by:

$$D = D_{po} \frac{A_p}{A_{po}} + D_f$$

$$= 9.5085 \frac{A_p}{A_{po}} + .4215$$

and from this the coefficient is computed

$$C_D = \frac{D}{q\ A} = \frac{D}{25.58 \times .460} = \frac{D}{11.75}$$

The variation of the predicted drag coefficient with changes of angle of attack are indicated in Table XVII.

However, since this coefficient of drag lies along the direction of the relative wind it is desirable to convert this into a coefficient of force C_c parallel with the longitudinal axis. Transformation of C_D and C_N into C_c is accomplished by Table XVIII which shows the values for several angles of attack of

---

[29] cf. ante., p. 32.

$$C_L = \frac{C_n - C_D \text{ Sin } \theta}{\text{Cos } \theta}$$

and

$$C_c = C_{Dp} \text{ Cos } \theta - C_L \text{ Sin } \theta$$

The values of C_c thus predicted are plotted on Figure 14. and dotted curve is drawn through the points.

It is apparent that the procedure for predicting the resistance of the body gives slightly conservative results, that is predicted drag is slightly greater than the resistance measured in the course of the wind tunnel tests.

It may be stated in general that the procedure, set forth here, for predicting aerodynamic coefficients of force and moment acting on bodies of revolution will yield values of C_N, C_M, and C_c slightly greater than those resulting from experimentation. Study of the comparison of predicted vs. experimentally determined coefficients, Figure 14., indicates a slightly greater departure of the predicted curves from the measured at large angles of attack. This trend is often observed in other analytical work and it is deemed to be logical in the present case.

CONCLUSIONS

The procedure for predicting aerodynamic coefficients of force and moment suggested here will expedite preparation of reasonably accurate predicted aerodynamic design data. This study has been hindered by a lack of experimental aerodynamic force and moment data for bodies of revolution of various shape. As stated previously, drag or resistance data for such bodies rarely indicates the variation with respect to angle of attack. Only one test of a spheroidal shape has been located. Furthermore, inertia coefficient data for cylinders, axis parallel to the flow, is entirely lacking and the available data for cylinders having hemispherical ends and pointed ends is considered to be unreliable.

Systematic wind tunnel tests of various ellipsoidal and cylindrical bodies of revolution should be conducted. Such tests would evaluate the aerodynamic forces and moments for cylinders and ellipsoids of several fineness ratios. Also accurate tests are needed to determine the inertia coefficients for cylinders having flat, hemispherical and pointed ends. The data resulting from such tests will make it possible to accurately predict aerodynamic coefficients of force and moment for bodies of revolution by means of the procedure described in this thesis.

BIBLIOGRAPHY

BIBLIOGRAPHY

Bairstow, L., Applied Aerodynamics, Second Edition. London: Longmans, Green and Company, 1939. 808 pp.

Durand, W. F., Editor, Aerodynamic Theory, 6 volumes. Berlin: Julius Springer, 1934.

Jones, B., Elements of Practical Aerodynamics, Second Edition. New York: John Wiley and Sons, Inc., 1939. 436 pp.

Jones, R., "The Distribution of Normal Pressures on a Prolate Spheroid", Technical Report of the Advisory Committee for Aeronautics (British) Reports and Memoranda Number 1061, 1926-27. 86 pp.

Karman, T. von, "Calculation of Pressure Distribution on Airship Hulls", National Advisory Committee for Aeronautics, Technical Memoranda Number 574, July 1930.

Lamb, Horace, Hydrodynamics, Fifth Edition. Cambridge: The University Press, 1930. 687 pp.

_____, "The Inertia-Coefficients of an Ellipsoid Moving in Fluid", Technical Report of the Advisory Committee for Aeronautics (British) Reports and Memoranda Number 623, Volume I, 1918-19, pp. 128-129.

Milliken, C. B., Aerodynamics of the Airplane. New York: John Wiley and Sons, Inc., 1941. 182 pp.

Mises, R. von, Theory of Flight. New York: McGraw-Hill Book Company, Inc., 1945. 629 pp.

Prandtl, L., "Applications of Modern Hydrodynamics to Aeronautics", National Advisory Committee for Aeronautics Technical Report Number 116, 1925.

Prandtl, L., Tietjens, O. J., Applied Hydro- and Aeromechanics. New York: McGraw-Hill Book Company, Inc., 1934.

_____, Fundamentals of Hydro and Aeromechanics, First Edition. New York: McGraw-Hill Book Company, Inc., 1934. 270 pp.

Theodoreson, T. and Garrick, I. E., "General Potential Theory of Arbitrary Wing Sections", National Advisory Committee for Aeronautics, Technical Report Number 452, 19 .

Upson, R. H. and Klickoff, W. A., "Application of Practical Hydrodynamics to Airship Design", National Advisory Committee for Aeronautics, Technical Report Number 405, 1931.

TABLES

TABLE I

Spheroidal Properties, L/D = 1.0

(1)	(2)	(3)	(4)	(5)	(6)	(7)	(8)
x	x^2	a^2-x^2	$y = \pm\sqrt{a^2 - x^2}$	$\tan\alpha = -x/\sqrt{a^2 - x^2} = -(1)/(4)$	α (degr)	$\sin\alpha$	$\cos\alpha$
$-1.0a$	$1.00a^2$	0	0	∞	90°	1.0000	0
$-.9a$	$.81a^2$	$.19a^2$	$.4359a$	2.0650	64.16	.9000	.4358
$-.8a$	$.64a^2$	$.36a^2$	$.6000a$	1.3333	53.13	.8000	.6000
$-.7a$	$.49a^2$	$.51a^2$	$.7141a$	.9803	44.43	.7001	.7262
$-.6a$	$.36a^2$	$.64a^2$	$.8000a$	.7500	36.90	.6004	.7997
$-.5a$	$.25a^2$	$.75a^2$	$.8660a$	.5774	30.00	.5000	.8660
$-.4a$	$.16a^2$	$.84a^2$	$.9165a$	.4364	23.54	.3982	.9160
$-.3a$	$.09a^2$	$.91a^2$	$.9539a$	.3145	17.56	.3017	.9534
$-.2a$	$.04a^2$	$.96a^2$	$.9798a$	.2041	11.53	.1982	.9798
$-.1a$	$.01a^2$	$.99a^2$	$.9950a$	.1005	5.73	.0997	.9950
0	0	a^2	a	0	0	0	1.0
$+.1a$	$.01a^2$	$.99a^2$	.9950	-.1005	174.27	.0997	-.9950
$+.2a$	$.04a^2$	$.96a^2$	$.9798a$	-.2041	168.47	.1982	-.9798
$+.3a$	$.09a^2$	$.91a^2$	$.9539a$	-.3145	162.44	.3017	-.9534
$+.4a$	$.16a^2$	$.84a^2$	$.9165a$	-.4364	156.46	.3982	-.9160
$+.5a$	$.25a^2$	$.75a^2$	$.8660a$	-.5774	150.00	.5000	-.8660
$+.6a$	$.36a^2$	$.64a^2$	$.8000a$	-.7500	143.10	.6004	-.7997
$+.7a$	$.49a^2$	$.51a^2$	$.7141a$	-.9803	135.57	.7001	-.7262
$+.8a$	$.64a^2$	$.36a^2$	$.6000a$	-1.3333	126.87	.8000	-.6000
$+.9a$	$.81a^2$	$.19a^2$	$.4359a$	-2.0650	115.84	.9000	-.4358
$+1.0a$	$1.00a^2$	0	0	∞	90°	1.0000	0

TABLE II

SPHEROIDAL PROPERTIES, L/D=2

(1) x	(2) $y = \pm \frac{1}{L/D}\sqrt{a^2-x^2}$ $\pm .5(4)$ of Table I	(3) $\tan\alpha = -\frac{1}{L/D}\frac{x}{\sqrt{a^2-x^2}}$ $+ -.5(5)$ of Table I	(4) α (degr.)	(5) $\sin\alpha$	(6) $\cos\alpha$	(7) $\sin 2\alpha$ Y = $2x(5)x(6)$	(8) $\sin 2\alpha$ = $(2)x(7)$
-1.0a	0	∞	90.00	1.0000	0	0	0
- .9a	.2179a	1.0325	45.92	.7182	.6957	1.000	.2179a
- .8a	.3000a	.6667	33.70	.5548	.8320	.921	.2763a
- .7a	.3570a	.4902	26.11	.4400	.8979	.790	.2820a
- .6a	.4000a	.3750	20.56	.3512	.9363	.657	.2628a
- .5a	.4330a	.2887	16.10	.2773	.9608	.532	.2300a
- .4a	.4582a	.2187	12.34	.2137	.9769	.417	.1910a
- .3a	.4769a	.1572	8.93	.1552	.9879	.307	.1464a
- .2a	.4899a	.1020	5.82	.1014	.9949	.202	.0988a
- .1a	.4975a	.0520	2.90	.0506	.9987	.101	.0502a
0	.5000a	0	0	.0000	1.0000	0	0
+ .1a	.4975a	- .0520	177.10	.0506	- .9987	- .101	-.0502a
+ .2a	.4899a	- .1020	174.18	.1014	- .9949	- .202	-.0988a
+ .3a	.4769a	- .1572	171.07	.1552	- .9879	- .307	-.1464a
+ .4a	.4582a	- .2187	167.66	.2137	- .9769	- .417	-.1910a
+ .5a	.4330a	- .2887	163.90	.2773	- .9608	- .532	-.2300a
+ .6a	.4000a	- .3750	159.44	.3512	- .9363	- .657	-.2628a
+ .7a	.3570a	- .4902	153.89	.4400	- .8979	- .790	-.2820a
+ .8a	.3000a	- .6667	146.30	.5548	- .8320	- .921	-.2763a
+ .9a	.2179a	-1.0325	134.08	.7182	- .6957	-1.000	-.2179a
+1.0a	0	∞	90.00	1.0000	0	0	0

TABLE III

Spheroildal Properties, L/D = 3.0

(1)	(2)	(3)	(4)	(5)	(6)	(7)	(8)
x	$\pm\frac{1}{L/D}\left(\sqrt{a^2-x^2}\right)$ = ±.333x(4) of Table I	$\tan\alpha = \frac{1}{L/D}\frac{x}{\sqrt{a^2-x^2}}$ =-.333x(5) of Table I	α (degr.)	Sin α	Cos α	Sin 2α =2x(5)x(6)	y Sin 2α =(2)x(7)
-1.0a	0	∞	90°	1.0000	0	0	0
- .9a	.1453a	.6883	34.54	.5670	.8237	.934	.1359a
- .8a	.2000a	.4444	23.96	.4220	.9138	.770	.1540a
- .7a	.2380a	.3268	18.10	.3107	.9505	.591	.1407a
- .6a	.2667a	.2500	14.04	.2426	.9701	.481	.1272a
- .5a	.2887a	.1925	10.90	.1891	.9820	.372	.1074a
- .4a	.3055a	.1455	8.22	.1430	.9897	.283	.0864a
- .3a	.3180a	.1048	5.98	.1042	.9947	.207	.0660a
- .2a	.3266a	.0680	3.90	.0680	.9977	.136	.0443a
- .1a	.3317a	.0335	1.90	.0332	.9995	.066	.0220a
0	.3333a	0	0	0	1.0000	0	0
+ .1a	.3317a	-.0335	178.10	.0332	- .9995	-.066	-.0220a
+ .2a	.3266a	-.0680	176.10	.0680	- .9977	-.136	-.0443a
+ .3a	.3180a	-.1048	174.02	.1042	- .9947	-.207	-.0660a
+ .4a	.3055a	-.1455	171.78	.1430	- .9897	-.283	-.0864a
+ .5a	.2887a	-.1925	169.10	.1891	- .9820	-.372	-.1074a
+ .6a	.2667a	-.2500	165.96	.2426	- .9701	-.481	-.1272a
+ .7a	.2380a	-.3268	161.90	.3107	- .9505	-.591	-.1407a
+ .8a	.2000a	-.4444	156.04	.4220	- .9138	-.770	-.1540a
+ .9a	.1453a	-.6883	145.46	.5670	- .8237	-.934	-.1359a
+1.0a	0	∞	90°	1.0000	0	0	0

$\frac{1}{L/D} = \frac{1}{3} = .3333$

TABLE IV

SPHEROIDAL PROPERTIES, L/D=4

(1) x	(2) $y=\pm\frac{1}{L/D}\sqrt{a^2-x^2}$ =.25 x (4) of Table I	(3) $\tan\alpha=\frac{-1}{L/D}\frac{x}{\sqrt{a^2-x^2}}$ =-.25 x(5) of Table I	(4) α (degr.)	(5) Sin α	(6) Cos α	(7) Sin 2α =2x(5)x(6)	(8) Y Sin 2α = (2)x(7)
-1.0a	0	∞	90°	1.0000	0	0	0
- .9a	.1090a	.5162	27.30	.4586	.8886	.815	.0889a
- .8a	.1500a	.3333	18.43	.3178	.9482	.602	.0904a
- .7a	.1785a	.2451	13.77	.2380	.9712	.462	.0825a
- .6a	.2000a	.1875	10.62	.1843	.9828	.362	.0724a
- .5a	.2165a	.1443	8.21	.1428	.9898	.282	.0610a
- .4a	.2291a	.1091	6.23	.1085	.9941	.216	.0495a
- .3a	.2385a	.0786	4.50	.0785	.9969	.156	.0372a
- .2a	.2449a	.0510	2.92	.0509	.9987	.102	.0249a
- .1a	.2487a	.0251	1.43	.0249	.9997	.048	.0119a
0	.2500a	0	0	0	1.0000	0	0
+ .1a	.2487a	- .0251	178.57	.0249	-.9997	-.048	- .0119a
+ .2a	.2449a	- .0510	177.07	.0509	-.9987	-.102	- .0249a
+ .3a	.2385a	- .0786	175.50	.0785	-.9969	-.156	- .0372a
+ .4a	.2291a	- .1091	173.77	.1085	-.9941	-.216	- .0495a
+ .5a	.2165a	- .1443	171.79	.1428	-.9898	-.282	- .0610a
+ .6a	.2000a	- .1875	169.38	.1843	-.9828	-.362	- .0724a
+ .7a	.1785a	- .2451	166.23	.2380	-.9712	-.462	- .0825a
+ .8a	.1500a	- .3333	161.57	.3178	-.9482	-.602	- .0904a
+ .9a	.1090a	- .5162	152.70	.4586	-.8886	-.815	- .0889a
+1.0a	0	∞	90°	1.0000	0	0	0

$\frac{1}{L/D} = \frac{1}{4} = .250$

TABLE V

SPHEROIDAL PROPERTIES, L/D = 4.5

(1)	(2)	(3)	(4)	(5)	(6)	(7)	(8)
x	$y=\pm\frac{D}{L}\sqrt{a^2-x^2}$	$\tan\alpha=\pm\frac{D}{L}\frac{x}{\sqrt{a^2-x^2}}$	α (degr.)	$\sin\alpha$	$\cos\alpha$	$\sin 2\alpha$	$y\sin 2\alpha$
	$=\pm.2222\times(4)$ of Table I	$=-.2222\times(5)$ of Table I				$=2\times(5)\times(6)$	$=(2)\times(7)$
-1.0a	0	∞	90°	1.0000	0	0	0
- .9a	.0969a	.4590	24.66	.4173	.9088	.7590	.0735a
- .8a	.1332a	.2965	16.52	.2843	.9587	.5450	.0726a
- .7a	.1585a	.2180	12.30	.2130	.9770	.4165	.0660a
- .6a	.1780a	.1667	9.47	.1645	.9864	.3241	.0577a
- .5a	.1925a	.1283	7.31	.1273	.9919	.2527	.0486a
- .4a	.2040a	.0969	5.53	.0963	.9953	.1920	.0391a
- .3a	.2120a	.0700	4.00	.0698	.9976	.1392	.0295a
- .2a	.2178a	.0454	2.60	.0454	.9990	.0907	.0197a
- .1a	.2210a	.0223	1.28	.0223	.9997	.0446	.0099a
0	0	0	0	0	1.0000	0	0
+ .1a	.2210a	.0223	178.72	.0223	-.9997	-.0446	-.0099a
+ .2a	.2178a	.0454	177.40	.0454	-.9990	-.0907	-.0197a
+ .3a	.2120a	.0700	176.00	.0698	-.9976	-.1392	-.0295a
+ .4a	.2040a	.0969	174.47	.0963	-.9953	-.1920	-.0391a
+ .5a	.1925a	.1283	172.69	.1273	-.9919	-.2527	-.0486a
+ .6a	.1780a	.1667	170.53	.1645	-.9864	-.3241	-.0577a
+ .7a	.1585a	.2180	167.70	.2130	-.9770	-.4165	-.0660a
+ .8a	.1332a	.2965	163.48	.2843	-.9587	-.5450	-.0726a
+ .9a	.0969a	.4590	155.34	.4173	-.9088	-.7590	-.0735a
+1.0a	0	∞	90°	1.0000	0	0	0

$$\frac{1}{L/D} = \frac{1}{4.5} = .2222$$

TABLE VI

SPHEROIDAL PROPERTIES, L/D=5

(1) x	(2) $y=\frac{1}{L/D}\sqrt{a^2-x^2}$ =.2 x(4) of Table I	(3) $\tan\alpha=\frac{x}{-\frac{1}{L/D}\sqrt{a^2-x^2}}$ =-.2x(5) of Table I	(4) α (degr.)	(5) Sin α	(6) Cos α	(7) $\sin 2\alpha$ Y = 2x(5)x(6)	(8) $\sin 2\alpha$ = (2)x(7)
-1.0a	0	∞	90°	1.0000	0	0	0
- .9a	±.0871a	.4130	22.44	.3817	.9243	.705	.0614a
- .8a	±.1200a	.2667	14.93	.2576	.9663	.497	.0596a
- .7a	±.1428a	.1961	11.10	.1925	.9813	.368	.0525a
- .6a	±.1600a	.1500	8.53	.1483	.9889	.293	.0469a
- .5a	±.1732a	.1155	6.60	.1149	.9934	.228	.0395a
- .4a	±.1833a	.0873	4.99	.0869	.9963	.173	.0318a
- .3a	±.1908a	.0629	3.60	.0628	.9980	.125	.0228a
- .2a	±.1960a	.0408	2.33	.0406	.9992	.081	.0159a
- .1a	±.1990a	.0201	1.15	.0201	.9998	.040	.0080a
0	±.2000a	0	0	0	1.0000	0	0
+ .1a	±.1990a	-.0201	178.85	.0201	-.9998	- .040	-.0080a
+ .2a	±.1960a	-.0408	177.67	.0406	-.9992	- .081	-.0159a
+ .3a	±.1908a	-.0629	176.40	.0628	-.9980	- .125	-.0228a
+ .4a	±.1833a	-.0873	175.01	.0869	-.9963	- .173	-.0318a
+ .5a	±.1732a	-.1155	173.40	.1149	-.9934	- .228	-.0395a
+ .6a	±.1600a	-.1500	171.47	.1483	-.9889	- .293	-.0469a
+ .7a	±.1428a	-.1961	168.10	.1925	-.9813	- .368	-.0525a
+ .8a	±.1200a	-.2667	165.07	.2576	-.9663	- .497	-.0596a
+ .9a	±.0871a	-.4130	157.56	.3817	-.9243	- .705	-.0614a
+1.0a	0	∞	90°	1.0000	0	0	0

$\frac{1}{L/D} = \frac{1}{5} = .200$

TABLE VII

SPHEROIDAL PROPERTIES, L/D = 7

(1)	(2)	(3)	(4)	(5)	(6)	(7)	(8)
x	$y = \pm \frac{D}{L}\sqrt{a^2-x^2}$ $\pm .143 \times$ (4) of Table I	$\tan\alpha = \frac{x}{\pm \frac{D}{L}\sqrt{a^2-x^2}}$ $= -.143(5)$ of Table I	α (degr.)	Sin α	Cos α	Sin 2α = $2x(5)x(6)$	y Sin 2α = (2)x(7)
-1.0a	0	∞	90°	1.0000	0	0	0
- .9a	.0623a	.2955	16.46	.2833	.9590	.5440	.0339a
- .8a	.0858a	.1909	10.80	.1874	.9823	.3682	.0316a
- .7a	.1020a	.1402	7.98	.1388	.9903	.2550	.0262a
- .6a	.1143a	.1072	6.12	.1066	.9943	.2120	.0243a
- .5a	.1239a	.0825	4.72	.0823	.9979	.1641	.0204a
- .4a	.1310a	.0623	3.56	.0621	.9980	.1240	.0162a
- .3a	.1362a	.0450	2.58	.0450	.9990	.0900	.0123a
- .2a	.1400a	.0292	1.67	.0292	.9996	.0585	.0082a
- .1a	.1423a	.0144	.83	.0145	.9999	.0290	.0041a
0	.1430a	0	0	0	1.0000	0	0
.1a	.1423a	-.0144	179.17	.0145	-.9999	-.0290	-.0041a
.2a	.1400a	-.0292	178.33	.0292	-.9996	-.0585	-.0082a
.3a	.1362a	-.0450	177.42	.0450	-.9990	-.0900	-.0123a
.4a	.1310a	-.0623	176.44	.0621	-.9980	-.1240	-.0162a
.5a	.1239a	-.0825	175.28	.0823	-.9979	-.1641	-.0204a
.6a	.1143a	-.1072	173.88	.1066	-.9943	-.2120	-.0243a
.7a	.1020a	-.1402	172.02	.1388	-.9903	-.2550	-.0262a
.8a	.0858a	-.1909	169.20	.1874	-.9823	-.3682	-.0316a
.9a	.0623a	-.2955	163.54	.2833	-.9590	-.5440	-.0339a
1.0a	0	∞	90°	1.0000	0	0	0

$$\frac{1}{L/D} = \frac{1}{7} = .143$$

TABLE VIII

SPHEROIDAL PROPERTIES, L/D=10

(1) x	(2) $y=\frac{1}{L/D\sqrt{a^2-x^2}}$ .10x(4) of Table I	(3) $\tan\alpha=\frac{-1}{L/D}\frac{x}{\sqrt{a^2-x^2}}$ =-.10(5) of Table I	(4) α (degr.)	(5) Sin α	(6) Cos α	(7) Sin2α Y =2x(5)x(6)	(8) Sin2α =(2)x(7)
-1.0a	0	∞	90.00	1.0000	0	0	0
- .9a	.0436a	.2065	11.67	.2023	.9793	.3960	.0172a
- .8a	.0600a	.1333	7.60	.1323	.9912	.2625	.0157a
- .7a	.0714a	.0980	5.60	.0976	.9952	.1945	.0139a
- .6a	.0800a	.0750	4.30	.0750	.9972	.1498	.0120a
- .5a	.0866a	.0577	3.30	.0576	.9983	.1151	.0100a
- .4a	.0916a	.0436	2.50	.0436	.9990	.0872	.0080a
- .3a	.0954a	.0314	1.80	.0314	.9995	.0628	.0060a
- .2a	.09798a	.0204	1.17	.0204	.9998	.0408	.0040a
- .1a	.0995a	.0100	.57	.0100	1.0000	.0200	.0020a
0	.1000a	0	0	0	1.0000	0	0
+ .1a	.0995a	-.0100	179.43	.0100	1.0000	-.0200	-.0020a
+ .2a	.09798a	-.0204	178.83	.0204	.9998	-.0408	-.0040a
+ .3a	.0954a	-.0314	178.20	.0314	.9995	-.0628	-.0060a
+ .4a	.0916a	-.0436	177.50	.0436	.9990	-.0872	-.0080a
+ .5a	.0866a	-.0577	176.70	.0576	.9993	-.1151	-.0100a
+ .6a	.0800a	-.0750	175.70	.0750	.9972	-.1498	-.0120a
+ .7a	.0714a	-.0980	174.40	.0976	.9952	-.1945	-.0139a
+ .8a	.0600a	-.1333	172.40	.1323	.9912	-.2625	-.0157a
+ .9a	.0436a	-.2065	168.33	.2023	.9793	-.3960	-.0172a
+1.0a	0	∞	90.00	1.0000	0	0	0

$\frac{1}{L/D} = \frac{1}{10} = .10$

TABLE IX

Y SIN2α CORRECTION FACTORS

(1) x	(2) Average Theory	(3) Average Exper.	(4) Ordinant Correction Factor (3)/(2)
-1.0a	0	0	1.0000
- .9a	.0955	.1000	1.0500
- .8a	.0955	.1000	1.0500
- .7a	.0888	.0940	1.0600
- .6a	.0763	.0820	1.0600
- .5a	.0648	.0700	1.0800
- .4a	.0510	.0560	1.1000
- .3a	.0386	.0410	1.0600
- .2a	.0143	.0150	1.0500
- .1a	.0050	.0050	1.0000
0	0	0	1.0000
+ .1a	.0050	.0050	1.0000
+ .2a	.0143	.0143	1.0000
+ .3a	.0386	.0376	.9500
+ .4a	.0510	.0472	.9250
+ .5a	.0648	.0498	.7700
+ .6a	.0763	.0507	.6650
+ .7a	.0888	.0532	.6000
+ .8a	.0955	.0554	.5800
+ .9a	.0955	.0597	.6250
+1.0a	0	0	1.0000

TABLE X

Distribution of Y $\sin 2\alpha$, Corrected

	(1)	(2)	(3)	(4)	(5)	(6)	(7)	(8)
	Ordinant Correction Factor (4) of Table IX	L/D=2.0 Y $\sin 2\alpha$ (1)x(8) of Table II	L/D=3.0 Y $\sin 2\alpha$ (1)x(8) of Table III	L/D=4.0 Y $\sin 2\alpha$ (1)x(8) of Table IV	L/D=4.5 Y $\sin 2\alpha$ (1)x(8) of Table V	L/D=5.0 Y $\sin 2\alpha$ (1)x(8) of Table VI	L/D=7.0 Y $\sin 2\alpha$ (1)x(8) of Table VII	L/D=10.0 Y $\sin 2\alpha$ (1)x(8) of Table VIII
-1.0a	1.000	0	0	0	0	0	0	0
- .9a	1.050	.2280a	.1425a	.0934a	.0772a	.0645a	.0356a	.0181a
- .8a	1.050	.2870a	.1618a	.0949a	.0763a	.0625a	.0332a	.0165a
- .7a	1.060	.2990a	.1491a	.0875a	.0700a	.0557a	.0278a	.0147a
- .6a	1.060	.2680a	.1350a	.0767a	.0613a	.0587a	.0258a	.0127a
- .5a	1.080	.2482a	.1161a	.0660a	.0525a	.0427a	.0222a	.0108a
- .4a	1.100	.2102a	.0950a	.0545a	.0431a	.0350a	.0178a	.0088a
- .3a	1.060	.1552a	.0700a	.0394a	.0313a	.0242a	.0130a	.0064a
- .2a	1.050	.1038a	.0465a	.0262a	.0207a	.0167a	.0086a	.0042a
- .1a	1.000	.0502a	.0220a	.0119a	.0099a	.0080a	.0041a	.0020a
0	1.000	0	0	0	0	0	0	0
.1a	1.000	-.0502a	-.0220a	-.0119a	-.0099a	-.0080a	-.0041a	-.0020a
.2a	1.000	-.0988a	-.0443a	-.0249a	-.0197a	-.0159a	-.0082a	-.0040a
.3a	.950	-.1391a	-.0627a	-.0354a	-.0280a	-.0216a	-.0170a	-.0057a
.4a	.925	-.1778a	-.0080a	-.0458a	-.0362a	-.0294a	-.0150a	-.0074a
.5a	.770	-.1770a	-.0828a	-.0470a	-.0374a	-.0304a	-.0157a	-.0077a
.6a	.665	-.1749a	-.0847a	-.0482a	-.0384a	-.0312a	-.0162a	-.0080a
.7a	.600	-.1691a	-.0844a	-.0495a	-.0396a	-.0315a	-.0157a	-.0083a
.8a	.580	-.1603a	-.0793a	-.0524a	-.0422a	-.0346a	-.0183a	-.0091a
.9a	.625	-.0850a	-.0555a	-.0555a	-.0460a	-.0384a	-.0212a	-.0107a
1.0a	1.000	0	0	0	0	0	0	0

TABLE XI

VARIATION OF $\frac{\pi AB}{2} \Sigma y \sin 2\alpha$ WITH FINENESS RATIO

(1)	(2)	(3)	(4)	(5)	(6)
L/D	$\Sigma y \sin 2\alpha$ (Integr. of Figure 7.)	A	B	$\frac{\pi AB}{2}$ = x(3)x(4)	$\frac{\pi AB}{2}\Sigma y \sin 2$ = (2) x (5)
2	$.0676a^2$	1.215	1.700	3.244	$.2193a^2$
3	$.0365a^2$	1.124	1.800	3.178	$.1160a^2$
4	$.0183a^2$	1.082	1.859	3.160	$.0578a^2$
4.5	$.0172a^2$	1.071	1.879	3.161	$.0544a^2$
5	$.0128a^2$	1.062	1.895	3.161	$.0405a^2$
7	$.0070a^2$	1.034	1.939	3.149	$.0220a^2$
10	$.0033a^2$	1.020	1.960	3.140	$.0104a^2$

$A = 1 + K_1$

$B = 1 + K_2$

K_1 and K_2 are Lamb's Inertia Coefficients

TABLE XII

DETERMINATION OF ANGLE OF ATTACK CORRECTION FACTOR, K_θ

(1) θ	(2) $\sin\theta$	(3) $\cos\theta$	(4) $\sin 2\theta$	(5) $q\frac{\pi AB}{2}\Sigma y \sin 2\alpha \times \sin 2\theta$ (lbs.) $= .118 \sin 2$	(6) N_M^x (Measured)	(7) $K_\theta = (5)/(6)$
0	0	1.0000	0	0	0	1.000
4	.0698	.9976	.1392	.0164	.0155	.945
6	.1045	.9945	.2080	.0257	.0267	1.039
10	.1736	.9848	.3419	.0403	.0564	1.400

where $a/b = 4.0$, $\pi\frac{AB}{2}\Sigma y \sin 2\alpha = .062a^2$ (reference, Figure 8.)

at $V = 40$ ft./sec., $q = 1/2\rho V^2 = 1/2 \times .002378 \times 40^2 = 1.902$ lbs./sq.in.

and $q\,\pi\frac{AB}{2}\Sigma y \sin 2\alpha = 1.902 \times .062a^2 = .118a^2 = .1180$

but $a = 1$ (for $L = 2$ feet)

---

[x] footnote 8 , p. 12

TABLE XIII

COMPARISON OF COMPUTED AND MEASURED

PITCHING MOMENT OF A PROLATE SPHEROID

L/D = 4.0

(1) $\pm\theta$	(2) Sin 2θ	(3) Moment M_o	(4) Measured Moment M_{oM}[30]	(5) % Measured Moment ((4)/(3))100
0	0	0	0	100.0
4	.1392	.0538	.0520	103.5
6	.2079	.0804	.0770	104.4
10	.3419	.1320	.1220	108.2
20	.6415	.2480	.2070	119.8

[30] Jones, R., "The Distribution of Normal Pressures on a Prolate Spheroid", R and M 1061 p.536

TABLE XIV

FORCE AND MOMENT COEFFICIENTS FOR A CYLINDRICAL BODY OF REVOLUTION IN THE NINE FOOT WIND TUNNEL

(1)	(2)	(3)	(4)	(5)
$\pm\theta$	$\sin\theta$	$\cos\theta$	C_L (Test Data)	C_D (Test Data)
0	0	1.0000	0	.840
3	.0523	.9986	.034	.860
6	.1045	.9945	.075	.905
9	.1564	.9877	.122	.958
12	.2079	.9781	.180	1.050

	(6)	(7)	(8)	(9)
$\pm\theta$	$C_L \sin\theta$ (4)x(2)	$C_L \cos\theta$ (4)x(3)	$C_D \sin\theta$ (5)x(2)	$C_D \cos\theta$ (5)x(3)
0	0	0	0	.840
3	.0018	.0339	.0450	.859
6	.0078	.0745	.0946	.900
9	.0191	.1205	.1499	.946
12	.0374	.1761	.2180	.978

$\pm\theta$	(10)	(11)	(12)	(13)	(14)
	C_N (7) + (8)	C_c (9) - (6)	C_{Ms} (Test Data)	$.074C_N$	$C_{M\frac{1}{2}}$ (12 - (13)
0	0	.8400	0	0	0
3	.0789	.8572	.015	.0058	.0092
6	.1691	.8922	.056	.0125	.0435
9	.2716	.9288	.109	.0201	.0889
12	.4256	.9407	.165	.0314	.1336

$C_N = C_L \cos\theta + C_D \sin\theta$

$C_c = C_D \cos\theta - C_L \sin\theta$

Test Velocity, V = 100 mph

$q = \frac{1}{2}\rho V^2 = 25.58$ lbs./sq. ft.

C_{Ms} = Moment Coefficient at Support

TABLE XV

PREDICTED NORMAL FORCE AND MOMENT COEFFICIENTS

(1)	(2)	(3)	(4)	(5)	(6)	(7)
$\pm\theta$	$\sin\theta$	$\cos\theta$	$\sin 2\theta$	K_θ From Table XII	C_N =.796x(4) x(5)	C_{Mo} = .4575 x(4)
0	0	1.0000	0	1.00	0	0
3	.0523	.9986	.1043	.95	$\pm$ .0790	$\pm$ .0478
6	.1045	.9945	.2080	1.08	$\pm$ .1785	$\pm$ .0950
9	.1564	.9877	.3090	1.32	$\pm$ .3240	$\pm$ .1414
12	.2079	.9781	.4060	1.53	$\pm$ .4930	$\pm$ .1858

TABLE XVI

DETERMINING THE PROJECTED FRONTAL AREA

	(1)	(2)	(3)	(4)	(5)	(6)
$\pm\theta$	$\sin\theta$	$\cos\theta$	$d\cos\theta$ = .765 x (2)	$\ell\sin\theta$ = 2.15 x (1)	b' = .5((3)+(4))	A_p = 1.202x(5)
0	0	1.0000	.765	0	.3825	.460
3	.0523	.9986	.763	.1125	.4378	.527
6	.1045	.9945	.760	.2247	.4923	.592
9	.1564	.9877	.755	.3365	.5458	.656
12	.2079	.9781	.748	.4465	.5973	.717

$$d = \frac{9.18}{12.0} = .765 \text{ ft.}$$

$$b = .765/2 = .3825 \text{ ft.}$$

$$= \frac{25.8}{12.0} = 2.15 \text{ ft.}$$

$$b' = \frac{1}{2}(d\cos\theta + \ell\sin\theta)$$

Projected Frontal Area:

$A_p = b\,b' = \times .3825\,b' = 1.202\,b'$

TABLE XVII

COMPUTATIONS OF THE PREDICTED DRAG COEFFICIENTS

	(1)	(2)	(3)	(4)
$\pm\theta$	A_p/A	D = ‡	C_D *	$C_D \cos\theta$ **
0	1.00	9.930	.845	.845
3	1.03	10.221	.860	.858
6	1.08	10.691	.910	.905
9	1.19	11.721	.998	.986
12	1.29	12.671	1.078	1.052

‡ $D = D_p \frac{A_p}{A} + D_f = 9.5085 \frac{A_p}{A} + .4215$

* $C_D = \frac{D}{q\,A} = \frac{D}{25.58 \times .46} = \frac{(2)}{11.75}$

** $C_D \cos\theta$ = (3) x (2) of Table

TABLE XVIII

CONVERSION OF C_N and C_D (Predicted) INTO C_c

$\pm\theta$	(1) C_N *	(2) $C_D \sin\theta$ **	(3) C_L ***	(4) $C_L \sin\theta$ x x	(5) C_c x x x
0	0	0	0	0	.845
3	.0790	.0449	.0342	.0018	.856
6	.1785	.0951	.0839	.0088	.896
9	.3240	.1560	.1700	.0266	.959
12	.4930	.2238	.2751	.0571	.995

* C_N, (6) of Table XV

** $C_D \sin$ = (3) of Table XVII x (1) of Table XVI

*** $C_L = \frac{C_N - C_D \sin\theta}{\cos\theta} = \frac{(1) - (2)}{(2) \text{ of Table XVI}}$

xx $C_L \sin$ = (3) x (1) of Table XVI

xxx $C_c = C_D \cos\theta - C_L \sin\theta$ = (4) Table XVII - (4)

FIGURES

FIGURE 1.

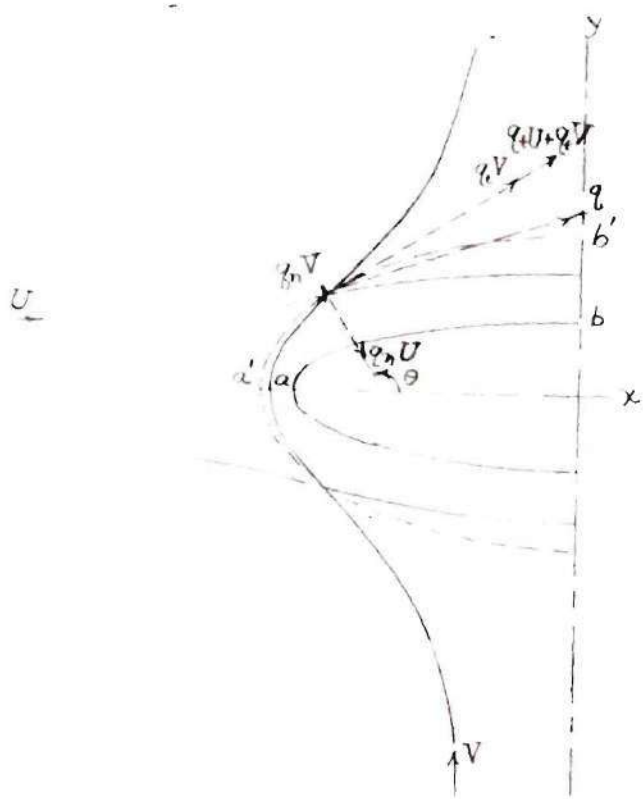

Prolate Spheroid in Oblique Flow

FIGURE 2.

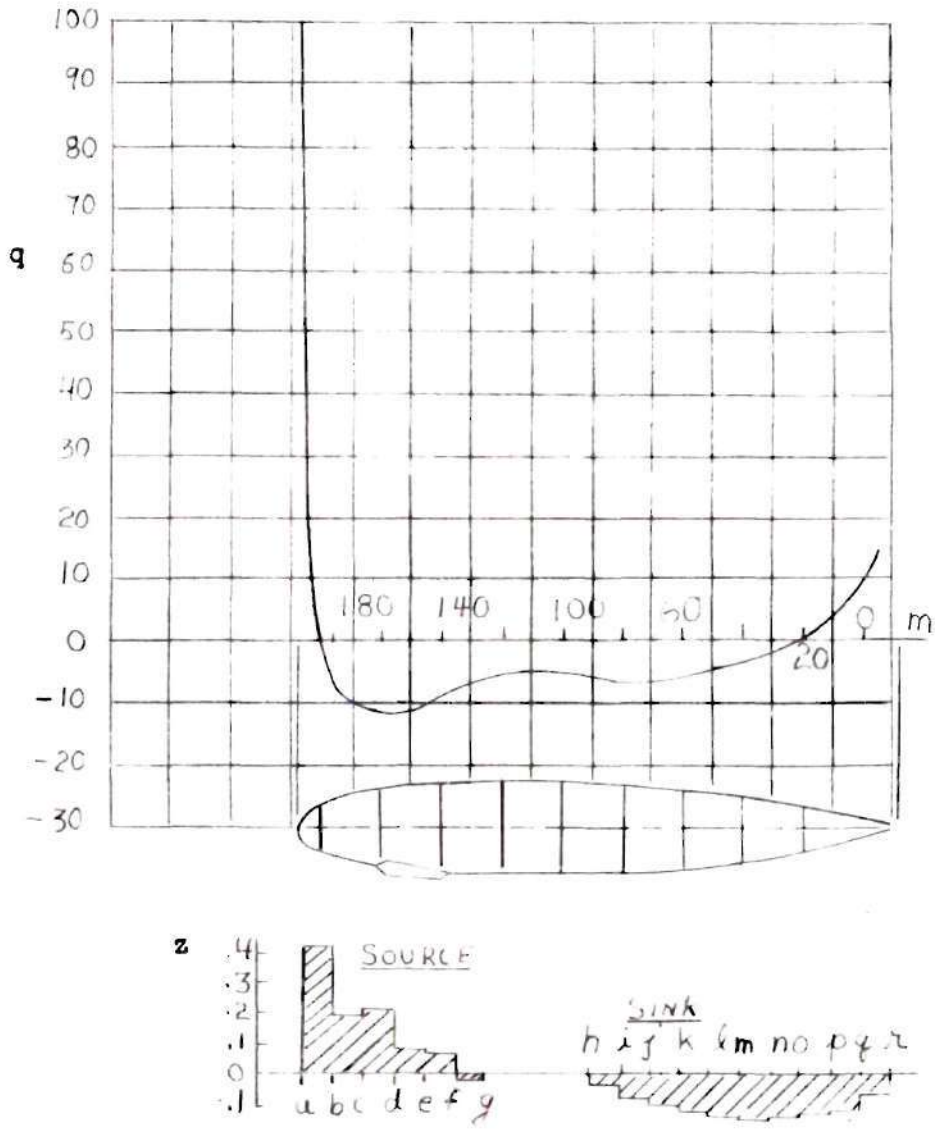

Karman's Method for Computing Pressure Distribution

FIGURE 3.

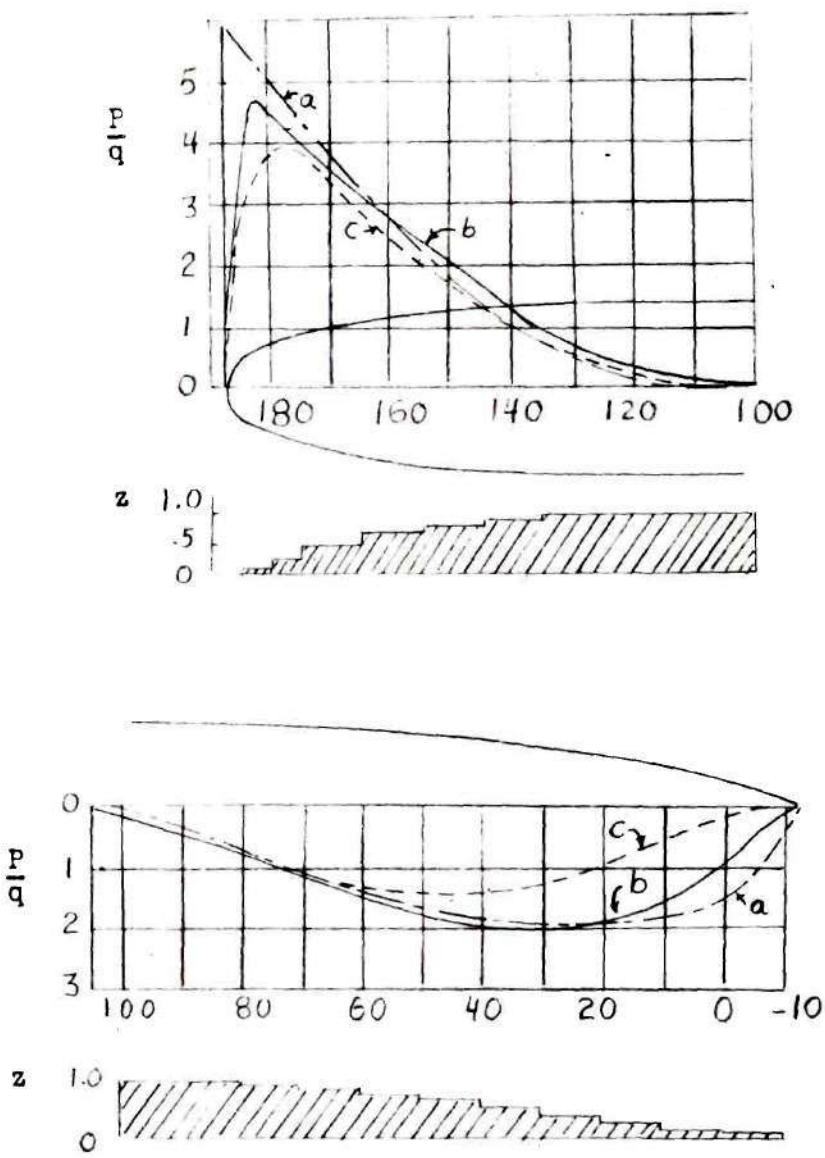

Karman's Method, Transverse Force Distribution

FIGURE 4.

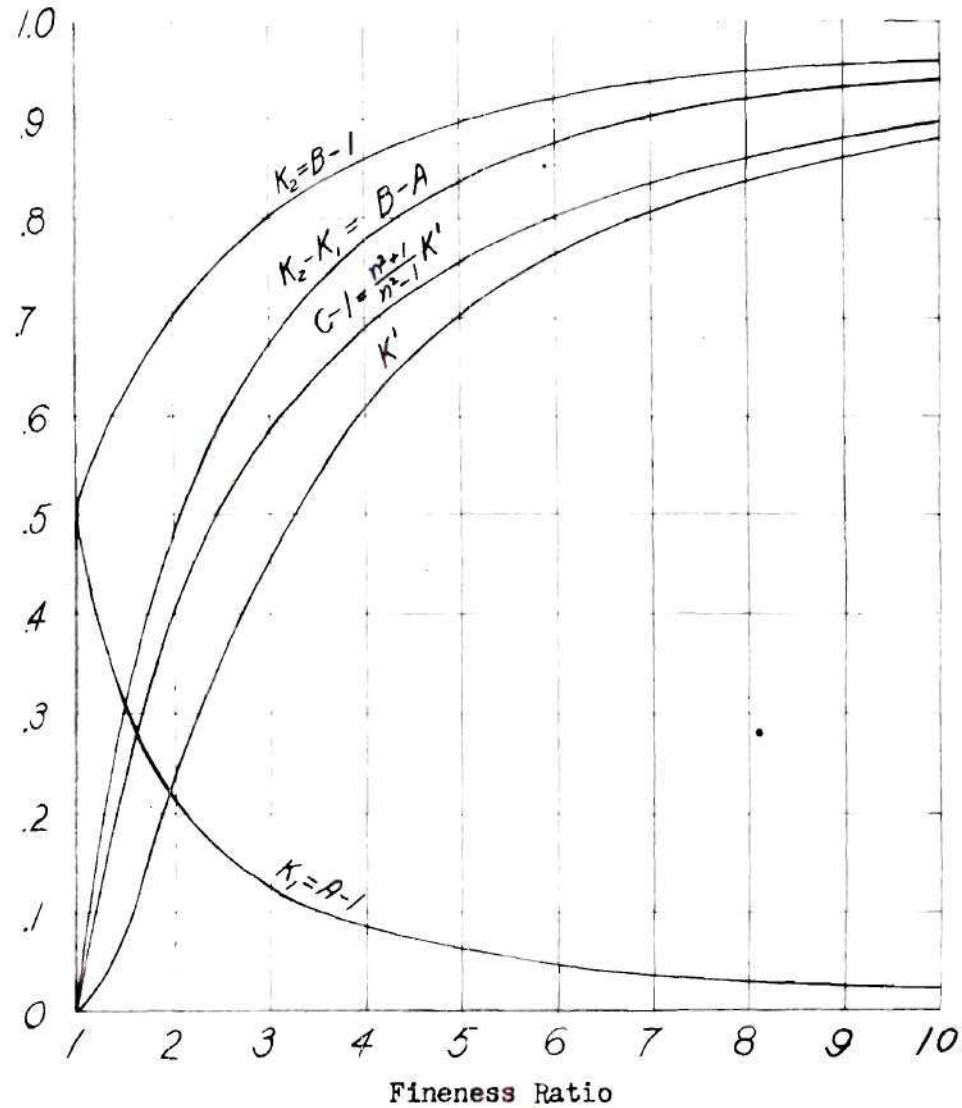

Lamb's Inertia Coefficient for the Prolate Spheroid

FIGURE 5.

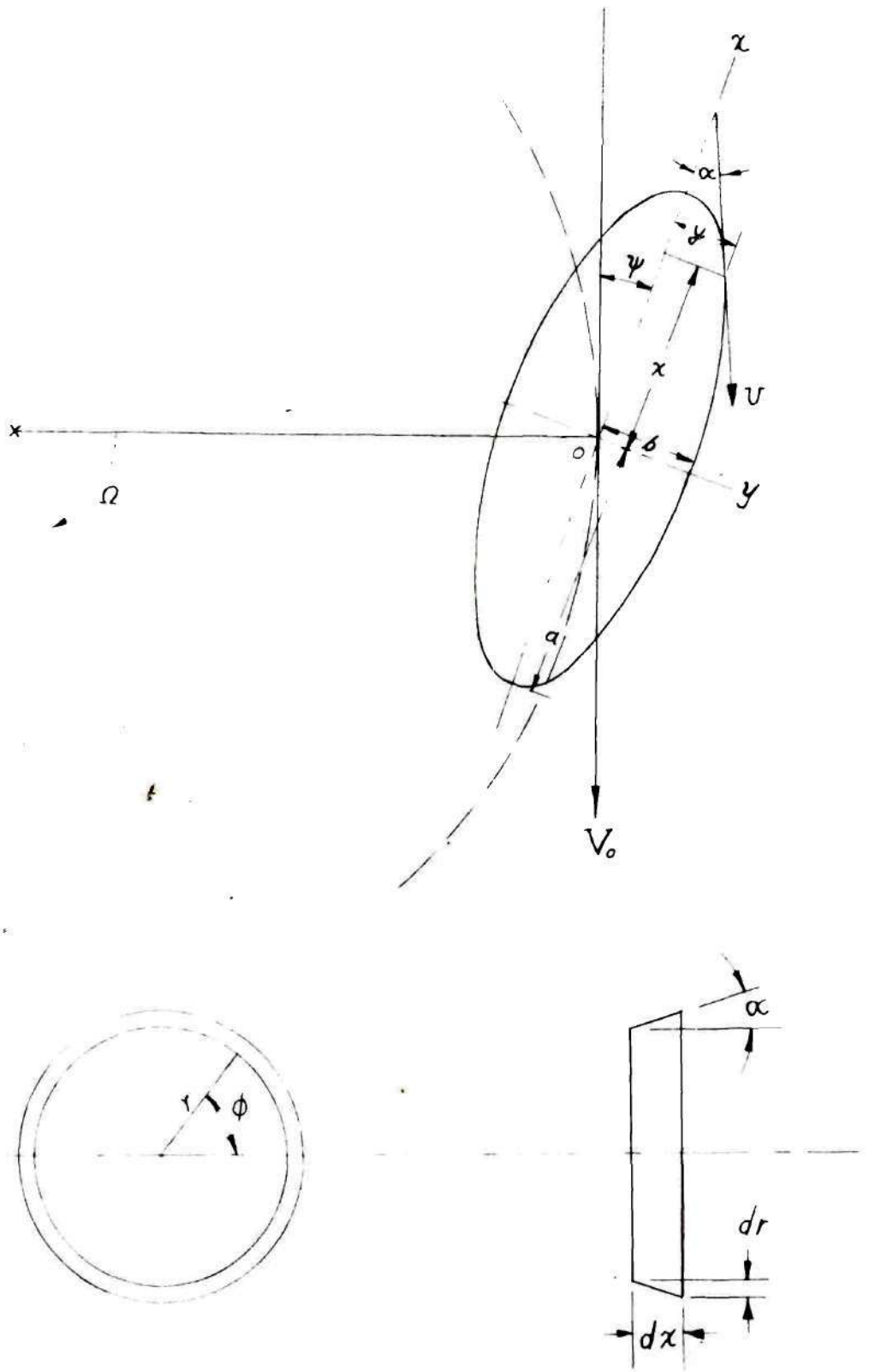

Symbols for the Prolate Spheroid Theories

FIGURE 6.

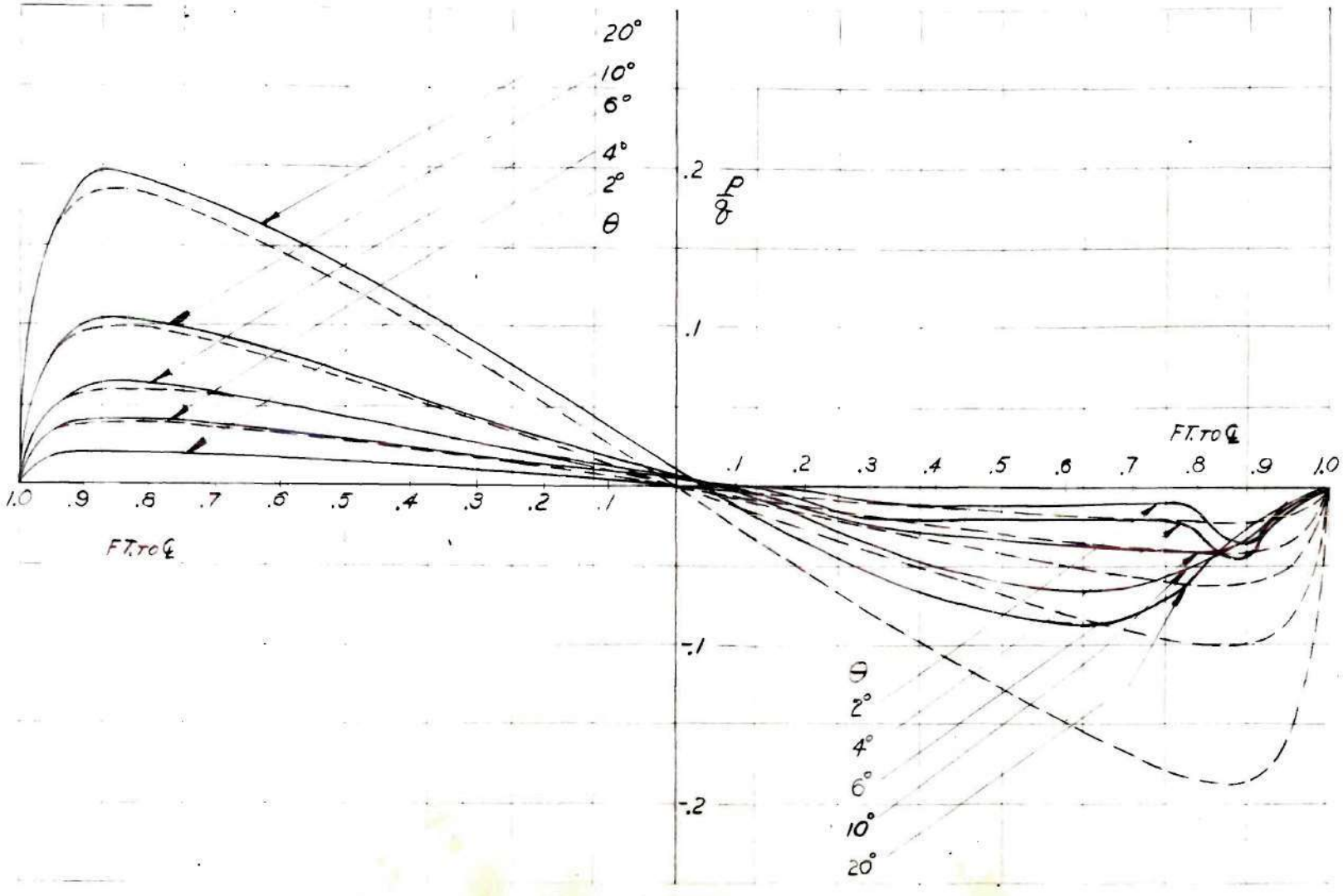

Comparison of Theoretical with Experimental
Transverse Force Distribution for Prolate Spheroids

FIGURE 7.

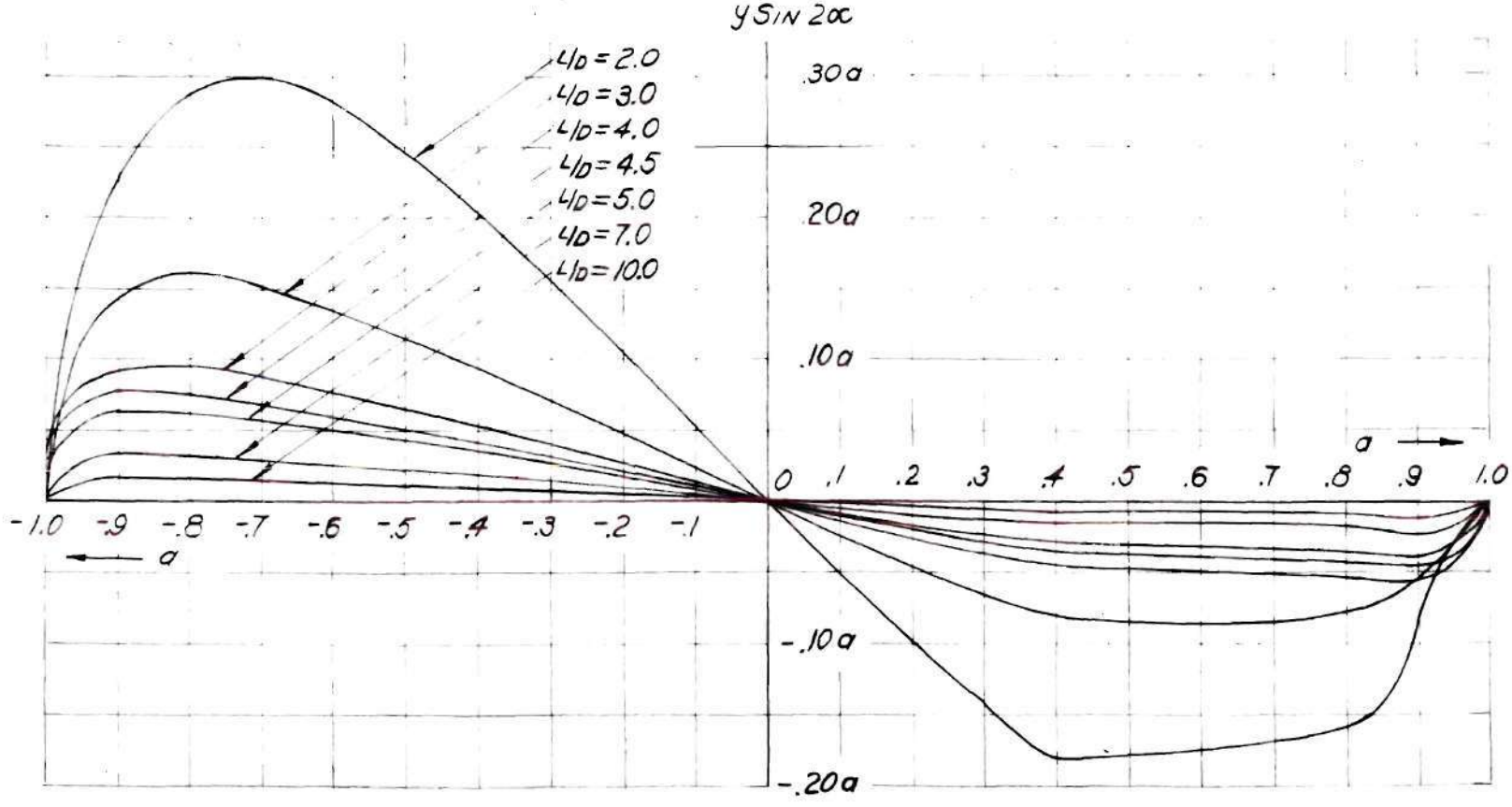

Distribution of y Sin 2α, Corrected

FIGURE 8.

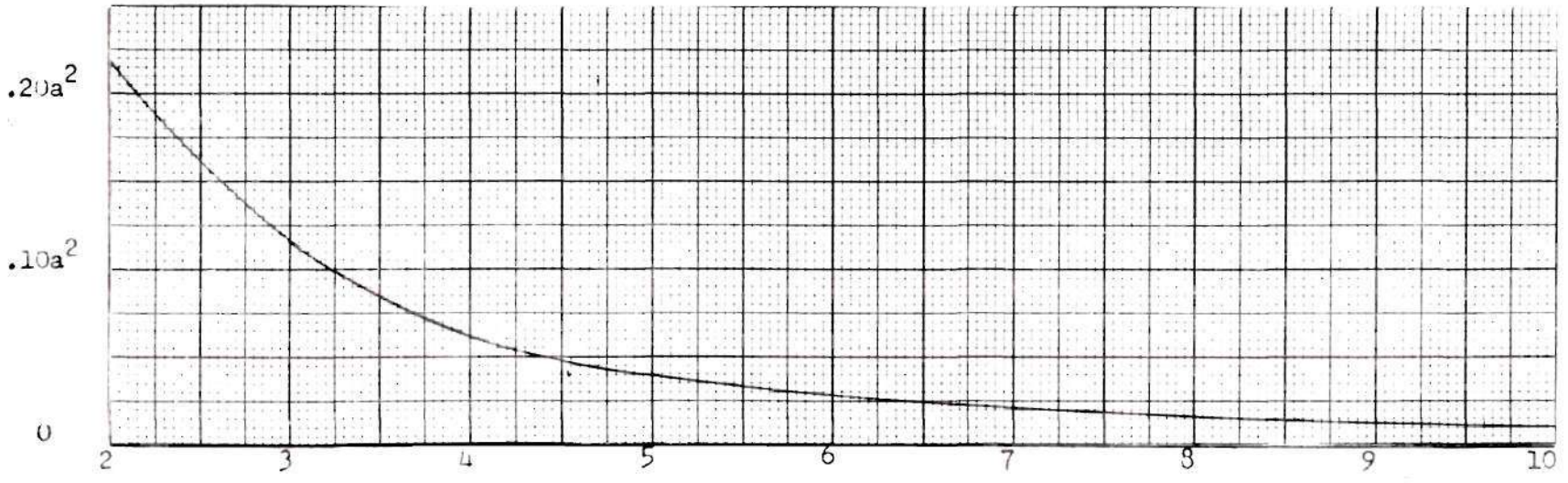

Variation of $\pi \frac{AB}{2} \Sigma$ y Sin 2 α

FIGURE 9.

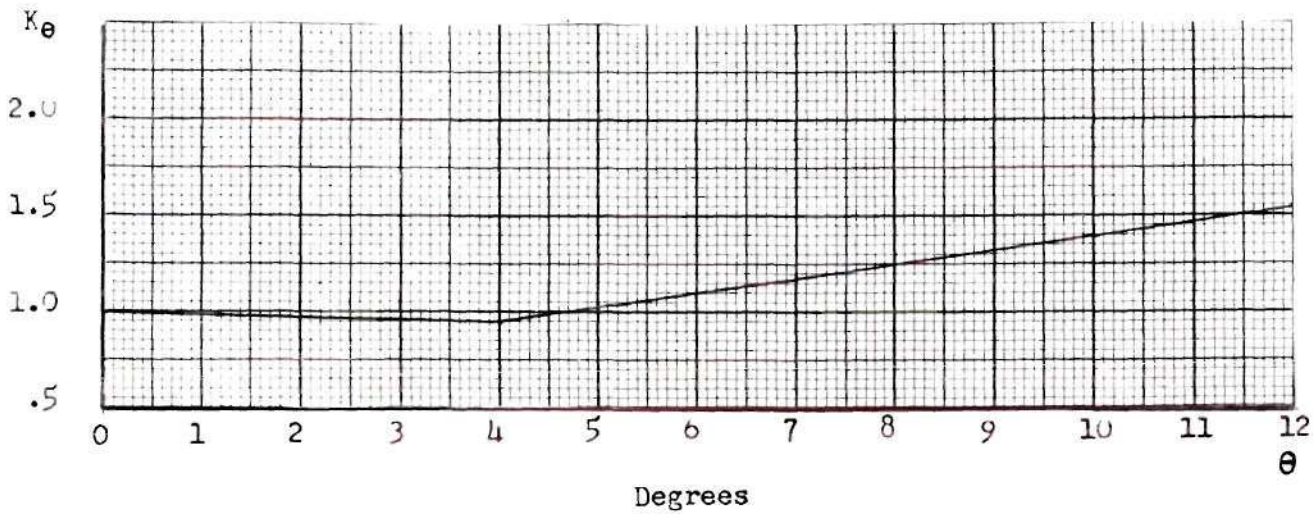

Angle of Attack Correction Factor, K_θ

FIGURE 10.

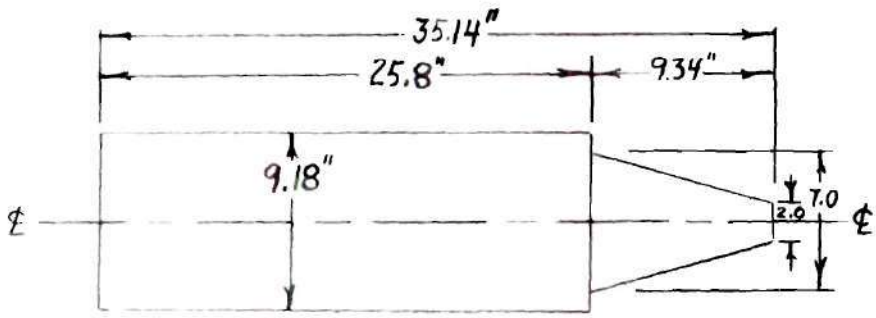

Body of Revolution
Tested in the Nine Foot Wind Tunnel

FIGURE 11.

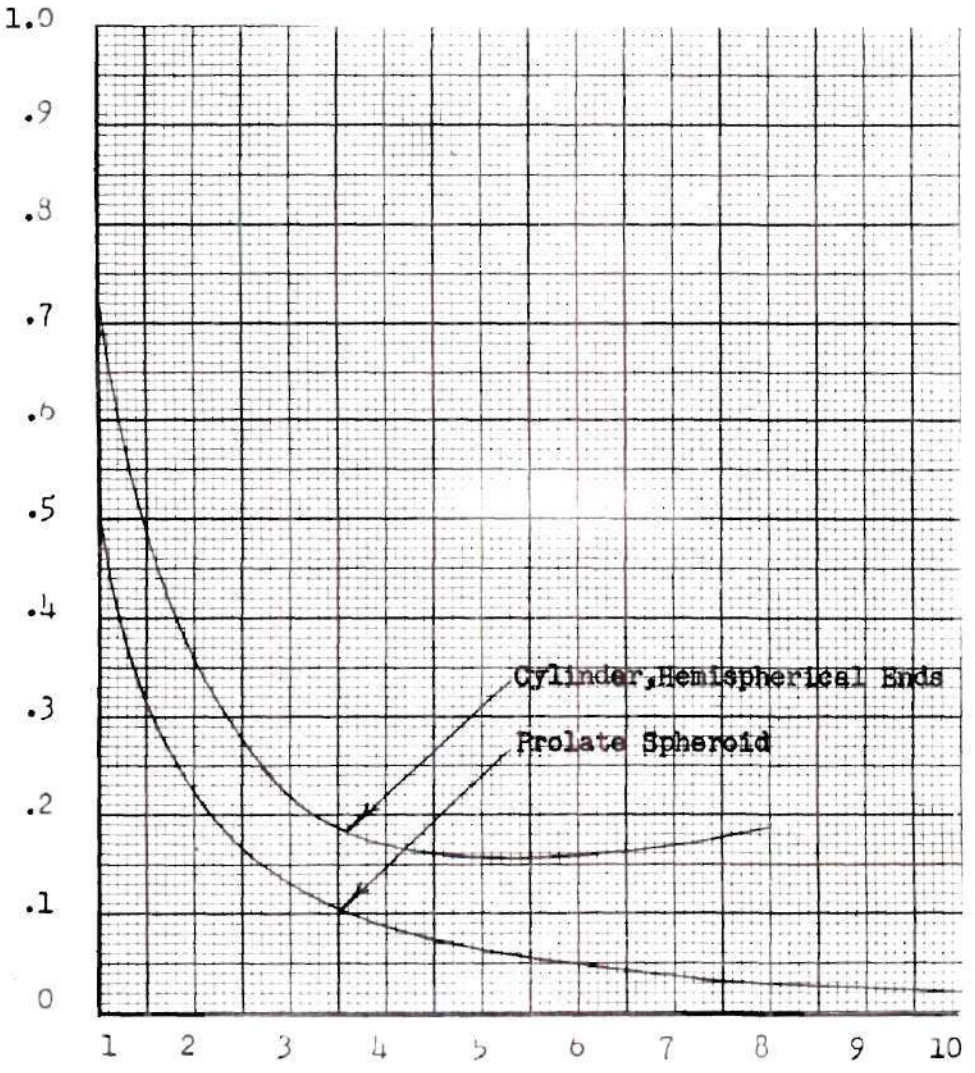

Comparison of Inertia Coefficients,
Prolate Spheroid with Cylinder

FIGURE 12.

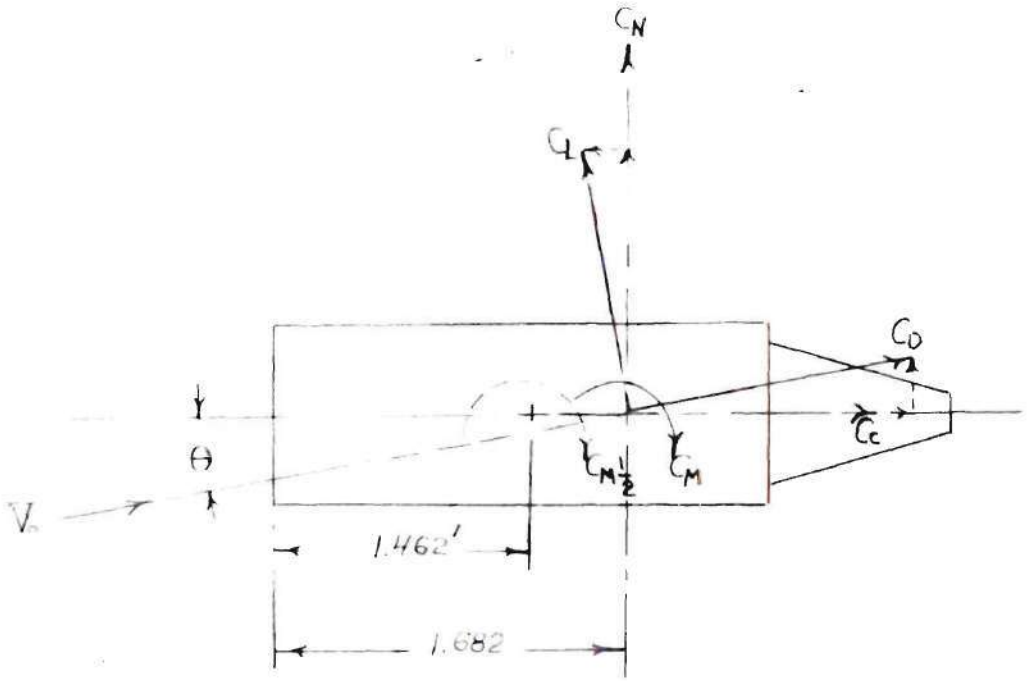

Force Diagram, Body of Revolution
Tested in Nine Foot Wind Tunnel

FIGURE 13.

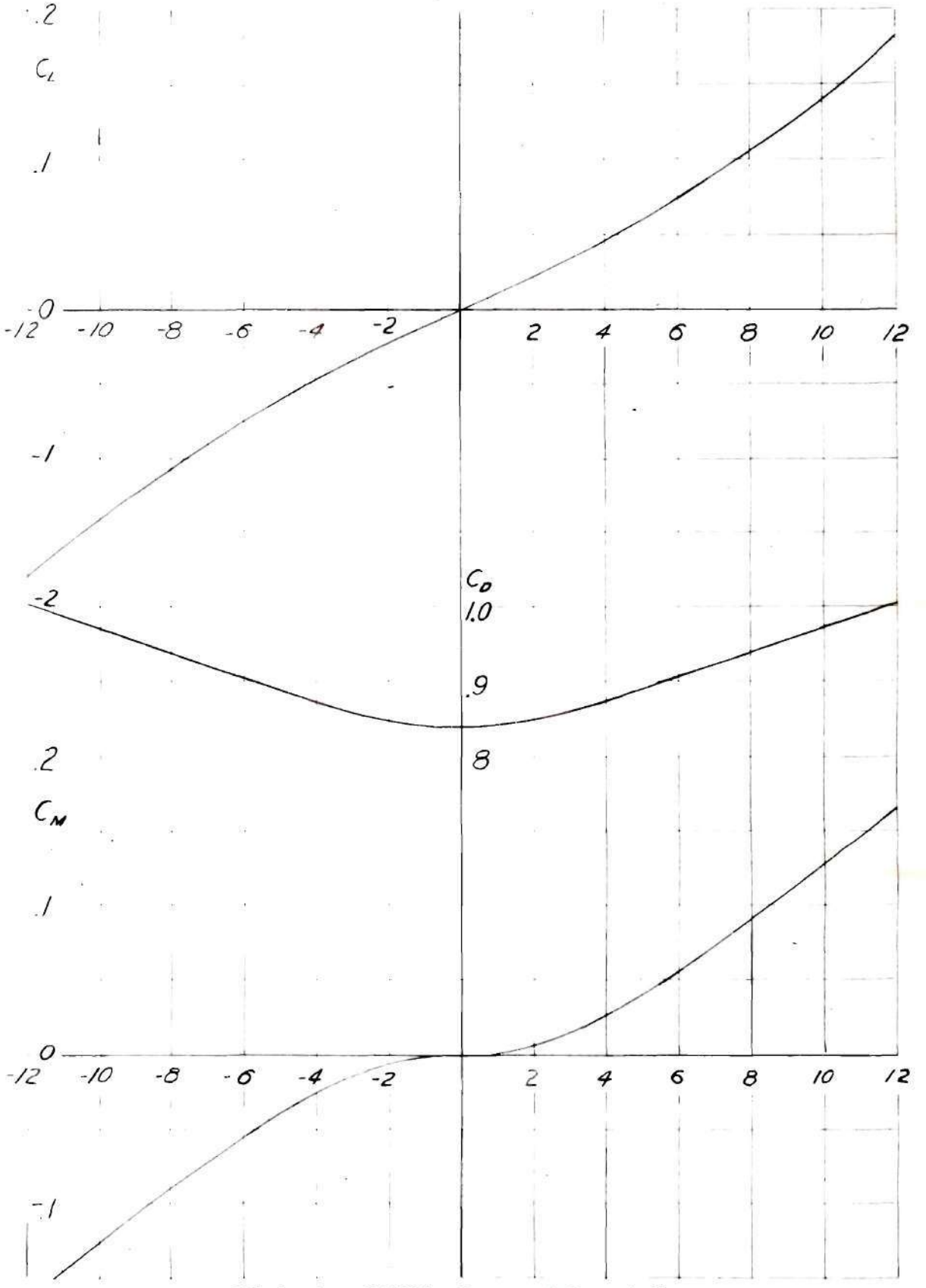

Coefficients of Lift, Drag and Moment for
Body of Revolution Tested in Nine Foot Wind Tunnel

FIGURE 14.

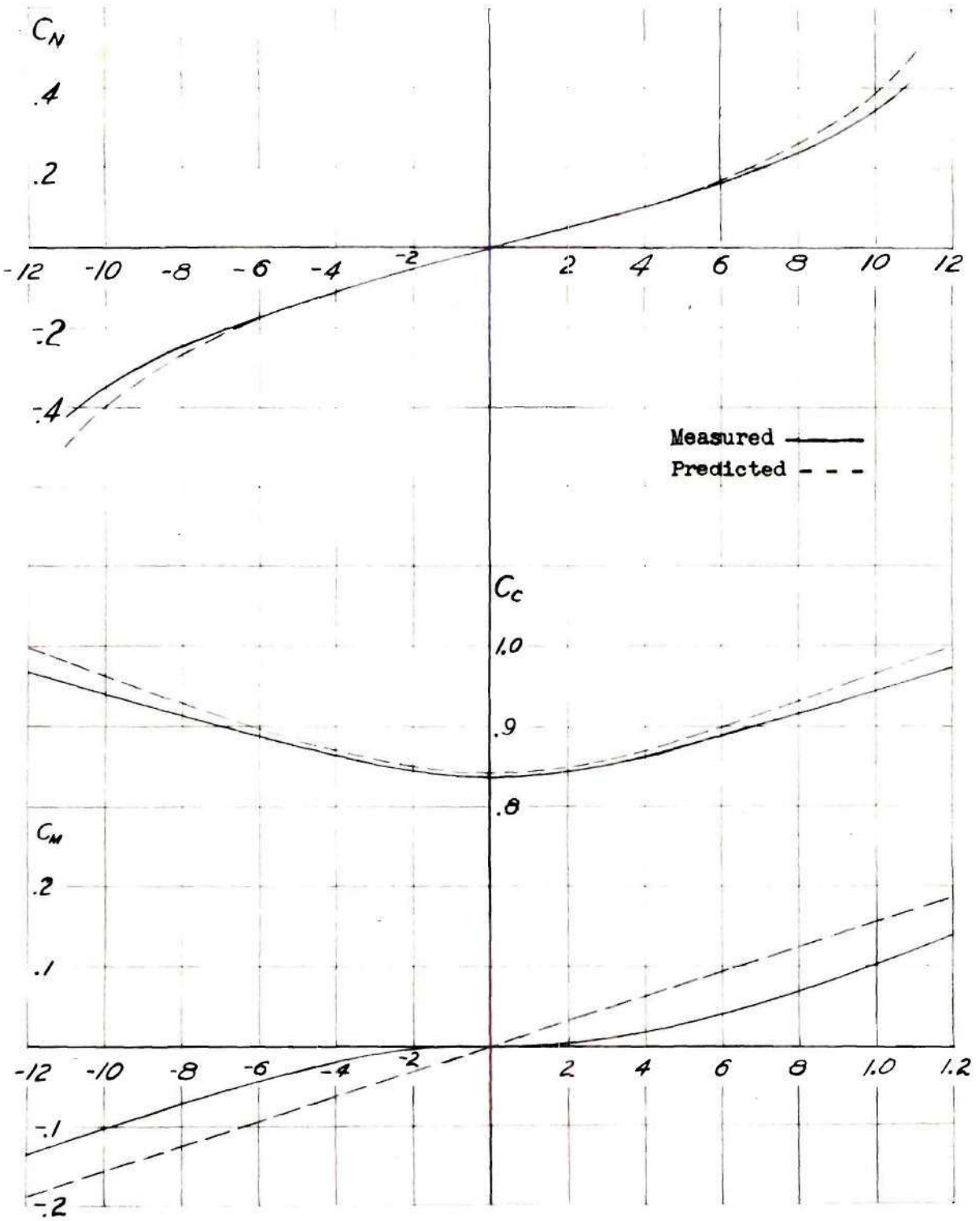

Comparison of Predicted with Measured Values of C_N, C_c, and C_D for Body of Revolution Tested in Nine Foot Wind Tunnel